Generation of transgene-free hematopoietic stem cells from human induced pluripotent stem cells

Olivier Piau, Mathias Brunet-Manquat, Laurence Petit, Bruno L'Homme, Brigitte Birebent, Christine Linard, Laetitia Moeckes, Thomas Zuliani, Hélène Lapillonne, Marc Benderitter, et al.

Generation of transgene-free hematopoietic stem cells from human induced pluripotent stem cells.

Olivier Piau[1,2,$], Mathias Brunet-Manquat[1,3,$], Bruno L'Homme[4], Laurence Petit[2], Brigitte Birebent[3], Christine Linard[4], Laetitia Moeckes[5], Thomas Zuliani[5], Hélène Lapillonne[1,6], Marc Benderitter[4], Luc Douay[6], Alain Chapel[1,4,§], Laurence Guyonneau-Harmand[1,3,§,*,#] and Thierry Jaffredo[3,§,*]

[1] Sorbonne Université, INSERM, Centre de Recherche Saint-Antoine, CRSA, F-75012 Paris, France.

[2]Sorbonne Université, CNRS UMR7622, Inserm U1156, Institut de Biologie Paris Seine, Laboratoire de Biologie du Développement/UMR7622, 9 Quai St-Bernard, 75005 Paris, France.

[3] EFS Ile de France, Unité d'Ingénierie et de Thérapie Cellulaire, Créteil, F-94017, France.

[4] Laboratoire de radiobiologie des expositions médicales (LRMed), Institut de Radioprotection et de Sûreté Nucléaire (IRSN), F-92262 Fontenay-aux-Roses, France.

[5] Etablissement Français du Sang – Atlantic Bio GMP – 2, rue Aronnax 44800 Saint-Herblain, France.

[6] AP-HP, Hôpital St Antoine/Trousseau, Service d'Hématologie Biologique, F- 75012 Paris, France.

*Correspondence to: laurence.harmand@upmc.fr; thierry.jaffredo@upmc.fr

[#]Lead Contact Laurence Guyonneau-Harmand; laurence.harmand@upmc.fr

[$]These authors contributed equally to this work

[§]Co-senior authors

SUMMARY:

Hematopoietic stem cells (HSCs) are the rare cells responsible for the lifelong curative effects of hematopoietic cell (HC) transplantation. The demand for clinical-grade HSCs has increased significantly in recent decades, leading to major difficulties in treating patients. A promising but not yet achieved goal is the generation of HSCs from pluripotent stem cells. Here, we have obtained vector- and stroma-free transplantable HSCs by differentiating human induced pluripotent stem cells (hiPSCs) using an original one-step culture system. After injection into immunocompromised mice, cells derived from hiPSCs settle in the bone marrow and form a robust multilineage, hematopoietic population that can be serially transplanted. Single cell RNA sequencing shows that this repopulating activity is due to a hematopoietic population that is transcriptionally similar to human embryonic aorta-derived HSCs. Overall, our results demonstrate the generation of HSCs from hiPSC and will help identify key regulators of HSC production during human ontogeny.

INTRODUCTION

Despite intensive efforts over the last decades, vector-free, transplantable human HSCs have not yet been successfully generated. In contrast, many blood cell types useful for human therapies have been efficiently generated from human embryonic stem cells (hESCs) or induced pluripotent stem cells (hiPSCs), including erythroid cells [1-4], B [5,6] and T cells [7-10], myeloid cells [11], megakaryocytes [12,13], or hematopoietic progenitor cells [14]. In recent years, many studies have sought to derive a population of $CD34^+CD45^+$ cells from pluripotent stem cells, with a phenotype approaching that of adult HSCs [15-19] used in clinical transplantation. These include reprogramming of adult cells by forced expression of transcription factors in fibroblasts [20] or endothelial cells [21]. However, these $CD34^+CD45^+$ populations have mainly demonstrated poor transplantation potential in immunocompromised mice, undermining therapeutic use. The only reports of successful generation of bona fide HSCs were obtained by redirecting hiPSC-derived or primary human endothelial cells with transcription factors [22-24]. However, the introduction of plasmids encoding oncogenes or the use of feeder cells precludes the use of these reprogrammed cells for clinical applications.

Interestingly, transplantable human HSCs can be obtained in teratomas, albeit with low frequency [25-27]. While not directly applicable to human therapy, this demonstrates that generation of HSCs from human pluripotent stem cells is possible and that cell-cell interactions play a key role in promoting self-renewal and multilineage repopulation activity [26]. Teratomas recapitulate some aspects of embryonic development. Although this has not been specifically investigated, the presence of HSCs argues for mechanisms reminiscent of early hematopoietic development. Indeed, the first transplantable HSCs arise from a specialized population of endothelial cells, namely hemogenic endothelial cells, formed early during embryonic development in the aorta-gonad-mesonephros (AGM) region [28,29], through an endothelial-hematopoietic transition (EHT) [30,31]. Some of these steps are likely recapitulated in embryoid body (EB) cultures that mimic events during hematopoiesis development. In particular, the formation of the hemogenic endothelium and budding of HCs are well documented [32-34].

Here, we describe a vector-free and stroma-free system for generating human HSCs capable of robust, long-term multipotent reconstitution and self-renewal *in vivo,* from hiPSCs. This protocol uses EB formation to generate a cell population resembling nascent HSCs found in the human embryonic AGM. Overall, our results demonstrate that the generation of feeder- and vector-free human HSCs is now feasible and is achieved by producing cells that more closely resemble the original HSCs that emerge during ontogeny.

RESULTS

Establishment of culture conditions

The optimal culture conditions to generate HSCs were established using a Design of Experiment approach (DOE). DOE is a statistical method for improving process performance by determining the optimal combination of input factors to optimize the output parameters, using the concept of desirability [35]. We first performed a literature review on *in vitro* HSC differentiation, amplification and maintenance (Figure 1). Then, an ensemble of 10 cytokines and growth factors reported to be important at different stages of mesoderm and hematopoietic specification [36-41] was defined. These cytokines and growth factors are (i) bone morphogenetic protein 4 (BMP-4), vascular endothelial growth factor (VEGF), and insulin-like

growth factor-1 (IGF-1), (ii) FMS-like tyrosine kinase ligand (FLT3-L), stem cell factor (SCF), interleukin-1 (IL1), interleukin-3 (IL3), interleukin-6 (IL6), granulocyte colony-stimulating factor (G-CSF), and thrombopoietin (TPO). The time frame of the protocol was set to 17 days (D17), according to Lengerke and colleagues [40]. We defined a concentration range for each of the cytokines as an input variable (Table S1). As output variables, we chose cell amplification, the frequency of long-term culture-initiating cells (LTC-ICs) and the expression of several surface markers associated with populations amenable to long-term transplantation, i.e., CD34, CD38, CD71, CD109, HLA-DR, CD90, CD33, CD13, CD117 (Table S1). The software defined sixteen different combinations, which were tested by measuring baseline variables (Table S1). These results were then subjected to regression analysis, and the response was plotted. The predictive model identified three efficient combinations of cytokines (Table S2). These three combinations were used to differentiate the FD136-25 and IMR90-16 hiPSC lines for 17 days. Each of the combinations triggered cell proliferation, low hematopoietic commitment ($CD34^+CD45^+$ and/or $CD117^+CD90^+$). Flow cytometric analysis of cell populations grown under the three conditions was performed using a panel of endothelial and hematopoietic-specific markers (Figure 1 and Table S2). Combination A showed the best ratio of immature ($CD34^+$, $CD43^+$, and $CD117^+$) to mature ($CD45^+$) hematopoietic markers. Differentiated FD136-25 cells were also grafted in irradiated NOD-SCID primary recipients (Figure 1 and Table S2). Combination A also showed the highest rate of human $CD45^+$ cells in NOD/SCID-LtSz-scid/scid (NOD/SCID) mice and was therefore selected for further use (Figure 1).

Long-term, multilineage repopulating activity and phenotypic analysis of the hematopoietic populations

While $CD34^+CD45^+$ HCs appeared to burst from embryoid bodies (EBs) at D10 to D14 in standard protocols for hiPSC differentiation, [18,22,40,42], the EBs in combination A at D17 remained compact and spherical without bursting, indicating a delay in differentiation (Figure 2A). The D17 EB hematopoietic repopulation potential was tested by transplanting 4.10^5 dissociated cells retro-orbitally into 8-week-old sublethally irradiated (2.4-3.5 Gy) NOD.Cg-PrkdcscidIl2rgtm1Wjl/SzJ (NSG) mice for 20 weeks (Figure 2A). The efficiency of reconstitution was systematically compared to that obtained with cord blood (CB)-derived $CD34^+$ cells. These culture conditions were reproducibly and successfully applied to four additional individual

hiPSC lines obtained with different reprogramming protocols (Figure 2A; Table S3, Materials and Methods), demonstrating the robustness of the method. The presence of human HCs in mouse bone marrow (BM) was monitored by flow cytometry, functional hematopoietic assays (T-cell activation and hemoglobin switch), cytological assays, RT-qPCR, and single-cell RNA sequencing (scRNA-Seq) (Table S3).

Primary NSG recipients transplanted with D17 cells derived from one or the other of the five hiPSC lines (Table S3) exhibited reconstitution of human hematopoietic cells (59/60), as shown by flow cytometric analysis of human (h) CD45 (Figure 2B) and surface expression of hCD34, hCD43, and hCD45 in mouse BMs (Figure 2C, D). The five hiPSC lines tested showed overall efficient hematopoietic reconstitution, with a mean of 4.1±0.6% $CD34^+$, 7.2±1.0% CD43+, and 13.3±1.5% $hCD45^+$ cells in mouse total mononucleated cells BM (Figure 2C, D). This is more than 130-fold the threshold of 0.1% $hCD45^+$ normally considered positive for transplantation of human HCs into NSG mice [43]. These grafting results were similar to those obtained with $CD34^+$ CB cells under the same conditions (Figure 2D). To test the robustness of the protocol, Pci-CAU hiPSCs were differentiated by an independent laboratory (Atlantic Bio GMP Platforme, Nantes; France), inoculated into irradiated NSG mice, and monitored over time for up to 20 weeks (Figure S1A-C). These cells showed robust engraftment and multilineage differentiation, similar to cells produced in the original laboratory (compare Figure S1C, 20 weeks with Figure 2D). This confirms the reproducibility of the protocol.

Twenty weeks after transplantation, the mouse BM harbors robust human myeloid, B- and T-lymphoid cells ($hCD33^+$, $hCD19^+$ and $hCD3^+$, respectively) and $hCD235a^+$ erythroid progenitors/precursors (Figure 2E) [44-46]. Figure 2F shows a representative cytometry analysis of BMs isolated from NSG primary recipients transplanted with D17 EB cells, mock-injected (saline, Figure S1D) or $CD34^+$ CB cells (Figure S1E). The D17 EB cells (Figure 2F) show a similar multilineage pattern as the $CD34^+$ CB cells (Figure S1E), including myeloid ($hCD14^+hCD15^+$), B lymphoid ($hCD19^+hIgM^+$), T lymphoid ($hCD3^+$) and red blood cells ($hCD71^+hCD235a^+$). We also analyzed the primitive $hCD34^+hCD38^+$ or $hCD38^-$ populations in the $hCD45^+$ cell population in 14 primary mice (2 independent series) inoculated with D17 EB cells. The total percentage of $hCD45^+$ cells was 5.2±1.5% (Figure S1F). The percentages of $hCD45^+hCD34^+hCD38^+$ cells were 4.9±0.7% and that of $hCD45^+hCD34^+hCD38^-$ cells was 0.5±0.2% (Figure S1G, H). These numbers

are consistent with works reporting transplantation of CD34$^+$ CB cells into NSG mice at 20 weeks of age [23, 47].

Peripheralization of the transplanted cells was confirmed by the presence of hCD45$^+$ cells in the circulating blood, which showed a multilineage pattern (Figure S1G) resembling that observed in the peripheral blood of CD34$^+$ CB transplanted recipients (Figure S1H), whereas no signal was found in mock-injected animals (Figure S1F). In the thymus, hCD3$^+$ cells showed TCRαβ expression greater than 60% and TCRγδ expression less than 30% (Figure 2G and S1I), a pattern consistent with that obtained with CD34$^+$ CB cells (Figure S1J) and confirming the presence of mature T cells as demonstrated by the expression of hCD4 and hCD8 (Figure 2G) [48]. In addition, hCD45$^+$ cells in the spleen were characterized by the presence of T and B cells expressing hTCRß and hCD19, respectively (Figure S1K), similar to CD34$^+$ CB grafts (Figure S1L). Figure 2H shows multilineage analysis of representative samples from three different graft series, demonstrating lineage variability between individuals.

Single-cell transcriptome and functional analysis of the grafted mouse BM

To get an unbiased view of the human cells in the mice BM after engraftment, we performed 10X Genomics on the BM of two representative primary mice (L5 and L1) 20 weeks after transplantation. As shown in Figure 3A-C and in Figure S2A, the BM of both recipients contained human erythroid, B, T, plasmacytoid dendritic, monocytic, and MAST cells (the strategy for distinguishing human and mouse cells is described in detail in the Materials and Methods section). The proportion of the different cell types was consistent between scRNA-Seq and FACS analysis and between the two mice (Figures 3D-F and Figure S2A-D). Human erythroid cells expressed □-, □-, □-, and □-globins, indicating mature erythropoiesis (Figure 3G).

To substantiate the functionality of the transplanted cells, we performed a human-selective clonogenic assay using BM cells isolated from primary recipients. We obtained an overall frequency of 17.5±2.4 colonies from 10^4 BM cells (Figure 4A), (to be compared with 19.2±3.8 colonies from 10^4 total BM cells obtained for the CD34 primary recipients). These colonies were divided into CFU-GEMM (Figure 4A and 4B1), BFU-E (Figure 4B2), and CFU-GM colonies (Figure 4B3). Cytological analysis of colonies revealed the presence of mature macrophages (Figure 4C1), histiomonocytes (Figure 4C2), and erythroblasts (Figure 4C3). We also analyzed the ability of human erythroid progenitor cells isolated from mouse BM to

undergo hemoglobin switching *in vivo* (n=3, 30 recipients). RT-qPCR analysis of total BM cells and erythroid colonies *in vitro* revealed high levels of human adult β- (39.51±4.95% and 28.91±2.43%, respectively) and foetal γ-(57.49±3.95% and 68.70±5.55%, respectively) globin gene expression, whereas embryonic ε-globin was dramatically reduced to 3.0±1.2% and 2.39±1.59% of total globin content, respectively (Figure 3D), consistent with the scRNA-seq analysis (Figure 3G). This is a hallmark of definitive erythropoiesis in the primary recipients and comparable to the globin content obtained during erythroid differentiation of $CD34^+$ CB cells *in vitro* (Figure 4D), except for a small amount of epsilon globin, which is present in colonies derived from BM cells. Similar results were found when we analyzed globin content of individual BFU-E from primary recipients transplanted with D17 EB cells (n=24) and BFU-E from $CD34^+$ CB cells (n=24) (Figure S3A).

As for the T lineage, BM had a significant proportion of $hCD3^+$ cells (Figure 2F), similar to the content of $hCD3^+$ cells found in the thymus (Figure 2G). In addition, thymus of the recipient mice contained significant amounts of $hCD4^-$ and $hCD8^+$ cells, together with TCRαβ expression combined to a low percentage of TCRγδ, the distribution of which being reminiscent of normal T lymphopoiesis (Figure 2G). We used a physiological method that can efficiently test T cell stimulation and proliferation [49]. The thymic hCD3 T cell population was CFSE labeled and stimulated by hCD3 and hCD28 (n=3, 30 thymuses). Cell numbers increased over the course of 5 days (Figure 4F) thereby demonstrating T cell activation and expansion. The presence of B and T cells was also confirmed by q-PCR of CD19 (B lymphocyte surface antigen B4) and TCF7 (Transcription Factor 7), respectively, in BM, thymus, and spleen (Figure S3B).

A hematopoietic progenitor cell assay revealed the presence of granulocytes and erythroblasts (Figure S3C). A TaqMan® RT-qPCR assay using the Human Hematopoiesis Array disclosed the presence of the canonical blood cell markers in the $CD45^+$ hematopoietic fraction of BM (Figure S3D). To estimate the number of functionally engrafting human HSCs, we performed a limiting dilution assay [50] in primary NSG recipients and estimated that one D17 cell out of 15,700 is a fully SCID-repopulating cell (Figure 3G, Table S4).

To confirm the presence of human self-renewing HSCs, secondary transplants (n=40, Table S3) were performed. For each primary recipient, one secondary recipient was engrafted

with half of the flushed BM corresponding to 7.10^6 BM cells (Figure 2A). Twenty weeks after transplantation, $hCD45^+$ cells accounted for 12.2±0.8% of mononucleated BM cells (Figure 5A, representative sample), 8.1±0.6% of $CD43^+$, and 4.8±0.6% of $CD34^+$ cells (Figure 5B), demonstrating their sustained reconstitution capacity. In 40 of 40 secondary mice receiving BM cells, hematopoietic reconstitution was comparable to the pattern obtained with secondary $CD34^+$ CB cell transplantation and did not differ between individual hiPSC lines (Figure 5C, D). Figure 5E shows the reconstitution of the different HC lineages analyzed by flow cytometry in representative BM samples from secondary mice transplanted with primary mouse BM cells that received D17 EB cells, saline injection (Figure S4A) or $CD34^+$ CB cells (Figure S4B).

The cloning efficiency of human colony-forming cells was 7.1±2.0 out of a total of 10^4 BM cells from secondary recipients transplanted with EB cell progeny and 11.0±2.9 out of a total of 10^4 mouse cells BM derived from secondary recipients transplanted with $CD34^+$ cells, indicating a robust and long-lasting self-renewal potential (Figure 5F). The cells generated human erythroid progenitors with hallmarks of definitive erythropoiesis, i.e., high levels of β- (36.61±5.86%) and γ-globin (61.39±4.86%), whereas ε-globin was drastically reduced to 2.1±1.1% of total globins (Figure 4D), as analyzed by RT-qPCR.

A successful three-round serial-transplant assay was performed in NOD-SCID mice with 4.10^5, 7.10^6 and 7.10^6 cells inoculated for primary, secondary and tertiary recipients respectively. All three tertiary-recipient mice exhibited multilineage engraftment at 12 weeks (Figure S4C, D, E), demonstrating that D17-EB-derived human HSCs display robust multilineage and self-renewal potential *in vivo*.

Functional, molecular and phenotypic identification of the EB cells.

To better document our differentiation procedure, we transcriptionally profiled EBs at 4 different time points, i.e., D13, D15, D17, and D19 of culture, using 10X Genomics scRNA-Seq (n=2 biological replicates per time point for a total of 26,027 cells). UMAP visualization of the merged datasets identified 27 different cell types distributed among three main UMAP branches corresponding to the three germ layers, i.e., ectoderm, mesoderm and endoderm,

and a fourth branch containing cells of the trophoblast lineage (Figure 6A and Figure S5). To better characterize the events leading to HSC development, we focused on the endothelial and HC clusters (Figure 6A, top left). As a first approach, we compared this cell subset with a published scRNA-Seq dataset from the human AGM region at Carnegie stage (CS) 16, the time of HSC development [51], (Figure 6B). Both data sets showed two types of vascular endothelial cells, an arterial-like $CD34^+$, $CDH5^+$, $HEY2^+$, $GJA5^+$ cluster and a venous-like $CD34^+$, $CDH5^+$, $NR2F2^+$, $APLNR^+$ cluster (Figure 6C, D). These data suggest that our differentiation procedure produces populations similar to those in the aorta of the human embryo when HSCs arise from the hemogenic endothelium.

To further explore this hypothesis, we examined the pattern of expression of MYB and RUNX1 by RT-qPCR and compared it with the profile obtained by scRNA-Seq (Figure 7A) from D13 to D17. An increase in their expression after D15 was observed by both methods. Flow cytometric analysis of endothelial markers (CD34, CDH5) showed a decrease in endothelial cells after D13 and the gradual appearance of the $PTPRC^+$ population between D15 and 17 (Figure 7B). We also tested the endothelial and hematopoietic capacity of EB cells at D13, 17, and 19 by dedicated assays *in vitro* (Figure S6). D15 EB cells showed a strong endothelial potential, as evidenced by the formation of pseudo microtubules (Figure S6A) [52], and a poor hematopoietic capacity as they were able to form only a few clonogenic colonies and had a very low frequency of LTC-ICs (Figure S6B-D). In contrast, D17 cells lost endothelial potential but increased their hematopoietic potential (Figure S6A-D). Thus D17 EB cells have the highest HSC potential, coherent with the onset of hematopoiesis. Immunostaining of sections of D17 EBs showed that endothelial $CDH5^+CD31^+$ cells and $NG2^+$ pericytes were distributed throughout the periphery of the EBs and absent from the center (Figure 7D, E, F, G), as assessed relative to the interior of this endothelium-rich outer region which is bordered by a ring of SMA^+cells (Figure 7G). Interestingly, clusters of $RUNX1^+$ endothelial and HCs were also identified (Figure 7F). This suggests that the periphery of EBs contains a dense vascular network in which there is likely a transition from endothelial cells to HCs, confirming the scRNA-Seq results.

Finally, we identified the subpopulations of HSCs produced. We projected the recently published six-gene signature and HSC score [53], which distinguishes human embryonic HSCs from hematopoietic progenitor cells, onto the scRNA-Seq hematopoietic clusters (Figure 6E).

Several RUNX1^{+} HOXA9^{+} MLLT3^{+} MECOM^{+} HLF^{+} SPINK2^{+} cells clustered into a candidate HSC subpopulation (Figure 6F). Refined comparisons with additional markers of human HSC ontogeny suggest that these candidate HSCs exhibit an intermediate phenotype between CS10 early AGM HSCs [54] and CS14-15 HSCs [53], with some early markers such as LIN28, GAD1, and FGF23 maintained alongside more mature markers such as HOXA9, PTPRC, and STAT5A (Table S8). Overall, the differentiation protocol presented here and applied to EBs appears to recapitulate human AGM formation and to give rise to HSCs with an early to intermediate AGM phenotype.

DISCUSSION

We successfully produced HSCs capable of long-term transplantation and self-renewal from hiPSCs using a combination of cytokines and growth factors, defined by DOE.

Importantly, this was achieved by a one-step, GMP-compliant, procedure, without the use of reprogramming vectors.

We used DOE to finely tune a combination and concentrations of cytokines and growth factors that enabled the formation of HSCs. The protocol is extremely robust, as HSCs with similar reconstitution potential, approaching the reconstitution potential of $CD34^+$ CB cells, were from five different hiPSC lines, regardless of the reprogramming method. A scaling-up of the protocol was successfully implemented since GMP-compliant batches of D17 cells have been produced with equal efficiency in an advanced therapy medicinal product platform (Atlantic Bio GMP Platform, Nantes; France). In conclusion, both the robustness and the reproducibility of this protocol meet the requirements of clinical applications.

According to scRNA-Seq data, we generate about 4.6% HCs at D17 and around 1 in 10,000 cells carries the six-gene signature of embryonic HSCs [53]. This is fully consistent with our limiting dilution experiments showing that 1 in 15,700 cells is an HSC. This highly efficient engraftment is in line with data showing that, although each human AGM contains only 1 or 2 HSCs, they exhibit a high repopulation capacity [55]. Similarly, our hiPSC-derived HSCs show a very robust reconstitution potential in multiple recipients with the full spectrum of hematopoietic lineages in BM, circulating blood, thymus, and spleen. In addition, no signs of leukemia or teratomas were observed in any of the transplanted mice.

The main issue with *de novo* generation of HSCs is the clonal reconstitution and the presence of multipotent progenitor cells instead of true HSCs. The latter is of particular concern because NSG mice are known to exhibit a B lymphoid bias [56-58]. Primary recipients show variable grafting patterns, both in terms of hCD45 expression and composition of the different HC lineages, and the secondary recipients show grafting patterns distinct from their primary counterparts. This argues against clonal reconstitution. In addition, individual BFU-E colonies performed from a single transplanted mouse BM showed different ratios of β-, γ-, and ε-globins. This suggests that erythropoiesis is maintained by multiple progenitor cells and not by a clonal mechanism.

ScRNA-Seq analysis of the D17 EBS reveals 2 major endothelial clusters: an arterial-like $GJA5^+$ cluster and a venous-like $APLNR^+$ cluster. These profiles are essentially the same as those described for the human CS16 embryo [51]. Interestingly, Calvanese and colleagues [53]

describe the hemogenic endothelium as GJA5+ in the aorta of the human CS14 embryo. In contrast, some cells of the APLNR$^+$ endothelial cluster colocalize with the HCs cluster, suggesting that the HSCs obtained are likely derived from an APLNR$^+$ hemogenic endothelium. This is consistent with other findings describing a possible switch in the identity of the hemogenic endothelium during development from a venous to an arterial phenotype between CS10 and CS13 [54]. Since EB-derived HSCs identified, thanks to the six-gene embryonic HSC signature [53], exhibit an intermediate phenotype between CS10 and CS14, it seems highly plausible that the hemogenic endothelium from which they arise also display an earlier phenotype than CS14. Overall, our protocol likely recapitulates the emergence of HSCs from the human AGM between CS10 and CS14.

Thus, the plasticity of the hemogenic endothelium phenotype argues for an important role of the microenvironment in HSC production. This is reminiscent of the protocols that have succeeded in generating functional HSCs from teratomas [25] [26]. These protocols have demonstrated that a variety of cell types from all germ layers can provide a rich microenvironment [27] for generating HSCs suitable for long-term transplantation. Indeed, HSC formation in the AGM is driven by signals from a variety of sources, including non-mesodermal tissues such as the sympathetic nervous system [59]. The diversity of communications between cell types in teratomas likely reflects these signals, which are sent from different tissues during development and are critical for HSC to be produced. Similarly, EBs contain cells from the ectoderm, endoderm, and mesoderm. This ensemble of cell types may form a rich, complex microenvironment critical for the formation of transplantable HSCs. This may explain why our protocol succeeds in generating HSCs with long-term transplantability, whereas most protocols using EBs report cells with short-term potential.

Limitation of the study

EBs harbor an ensemble of cell types that may serve as a microenvironment. We do not yet know what type of tissue, cell type, and molecular interactions are required to promote HSC formation, but investigations are ongoing.

In the near future, it will be necessary to find markers for enrichment in endothelial/hematopoietic lineages if HSCs are to be generated for clinical translation. These approaches are currently under investigation.

Granulocytes and neutrophils are difficult to detect under our experimental conditions because samples are not processed immediately after collection and RNA content is low and RNases are relatively high, resulting in fewer transcripts detected and fewer usable sequencing reads using 10X technology.

We do not know whether the transplanted HSCs require non-hematopoietic tissue to develop in the mouse BM. A time course analysis of the transplanted non-hematopoietic tissues is underway.

Such a transgene- and feeder-free tool could pave the way for future clinical applications and the discovery of therapeutic targets by providing a model for deciphering the emergence of hereditary blood malignancies. Our system is also a real step towards a better understanding of developing hematopoiesis in the human embryo, as it can overcome the ethical constraints associated with human embryo research.

AUTHOR CONTRIBUTIONS

L.G.H., OP, and MBM performed the experiments with assistance from LP, BL, BB, and CL. OP performed the single-cell transcriptome analysis. TZ and LM replicated the culture protocol independently in an ATMP platform. LP replicated the FACS analysis independently. H.L., L.D., and A.C. helped with the design of the study. M.B. helped design the animal study. A.C., T.J., and L.G.H. monitored the study. L.G.H. and T.J. designed the study, analyzed the data, interpreted the experiments, and wrote the manuscript.

ACKNOWLEDGMENTS

We thank S. Viville (IGBMC, Strasbourg, France) and L. David (ISPCDC, Nantes, France) for providing iPS lines, Rima Haddad for scientific support and Sophie Gournet for excellent drawing assistance. This work benefited from equipment and services from the iGenSeq core facility, at ICM. We warmly thank F. Letourneur (Plateforme génomique Institut Cochin Paris) and to Y. Marie (Plateforme Génomique ICM) for help in single-cell sequencing and demultiplexing. Part of the bioinformatics analyses was performed on the Core Cluster of the Institut Français de Bioinformatique (IFB) (ANR-11-INBS-0013). We are indebted to the Fondation Ramsay Santé and Assistance Publique-Hôpitaux de Paris for providing the cord blood cells. This research was funded by the ANR-13-ASTR-009 “GIPSI” and ANR-19-ASMA-0005 “RESCUE” from the Direction Générale de l’Armement via the ASTRID/ANR program for AC, the ANR-20-CE17-0032-01 “HEMPLUS”, the FRM grant EQU201903007867 for TJ and the Etablissement Français du Sang via the APR 2013 for LGH.

Declaration of interest

The authors declare no competing interest

Inclusion and diversity

We support inclusive, diverse, and equitable conduct of research.

REFERENCES

1. Lu, S.J., Feng, Q., Park, J.S., and Lanza, R. (2010). Directed differentiation of red blood cells from human embryonic stem cells. Methods Mol Biol *636*, 105-121. 10.1007/978-1-60761-691-7_7.
2. Lapillonne, H., Kobari, L., Mazurier, C., Tropel, P., Giarratana, M.C., Zanella-Cleon, I., Kiger, L., Wattenhofer-Donze, M., Puccio, H., Hebert, N., et al. (2010). Red blood cell generation from human induced pluripotent stem cells: perspectives for transfusion medicine. Haematologica *95*, 1651-1659. 10.3324/haematol.2010.023556.
3. Hirose, S., Takayama, N., Nakamura, S., Nagasawa, K., Ochi, K., Hirata, S., Yamazaki, S., Yamaguchi, T., Otsu, M., Sano, S., et al. (2013). Immortalization of erythroblasts by c-MYC and BCL-XL enables large-scale erythrocyte production from human pluripotent stem cells. Stem Cell Reports *1*, 499-508. 10.1016/j.stemcr.2013.10.010.
4. Kurita, R., Suda, N., Sudo, K., Miharada, K., Hiroyama, T., Miyoshi, H., Tani, K., and Nakamura, Y. (2013). Establishment of immortalized human erythroid progenitor cell lines able to produce enucleated red blood cells. PLoS One *8*, e59890. 10.1371/journal.pone.0059890.
5. Carpenter, L., Malladi, R., Yang, C.T., French, A., Pilkington, K.J., Forsey, R.W., Sloane-Stanley, J., Silk, K.M., Davies, T.J., Fairchild, P.J., et al. (2011). Human induced pluripotent stem cells are capable of B-cell lymphopoiesis. Blood *117*, 4008-4011. 10.1182/blood-2010-08-299941.
6. French, A., Yang, C.T., Taylor, S., Watt, S.M., and Carpenter, L. (2015). Human induced pluripotent stem cell-derived B lymphocytes express sIgM and can be generated via a hemogenic endothelium intermediate. Stem Cells Dev *24*, 1082-1095. 10.1089/scd.2014.0318.
7. Galic, Z., Kitchen, S.G., Kacena, A., Subramanian, A., Burke, B., Cortado, R., and Zack, J.A. (2006). T lineage differentiation from human embryonic stem cells. Proc Natl Acad Sci U S A *103*, 11742-11747. 10.1073/pnas.0604244103.
8. Nishimura, T., Kaneko, S., Kawana-Tachikawa, A., Tajima, Y., Goto, H., Zhu, D., Nakayama-Hosoya, K., Iriguchi, S., Uemura, Y., Shimizu, T., et al. (2013). Generation of rejuvenated antigen-specific T cells by reprogramming to pluripotency and redifferentiation. Cell Stem Cell *12*, 114-126. 10.1016/j.stem.2012.11.002.
9. Themeli, M., Kloss, C.C., Ciriello, G., Fedorov, V.D., Perna, F., Gonen, M., and Sadelain, M. (2013). Generation of tumor-targeted human T lymphocytes from induced pluripotent stem cells for cancer therapy. Nat Biotechnol *31*, 928-933. 10.1038/nbt.2678.
10. Vizcardo, R., Masuda, K., Yamada, D., Ikawa, T., Shimizu, K., Fujii, S., Koseki, H., and Kawamoto, H. (2013). Regeneration of human tumor antigen-specific T cells from iPSCs derived from mature CD8(+) T cells. Cell Stem Cell *12*, 31-36. 10.1016/j.stem.2012.12.006.
11. Haruta, M., Tomita, Y., Yuno, A., Matsumura, K., Ikeda, T., Takamatsu, K., Haga, E., Koba, C., Nishimura, Y., and Senju, S. (2013). TAP-deficient human iPS cell-derived myeloid cell lines as unlimited cell source for dendritic cell-like antigen-presenting cells. Gene Ther *20*, 504-513. 10.1038/gt.2012.59.
12. Takayama, N., Nishikii, H., Usui, J., Tsukui, H., Sawaguchi, A., Hiroyama, T., Eto, K., and Nakauchi, H. (2008). Generation of functional platelets from human embryonic stem cells in vitro via ES-sacs, VEGF-promoted structures that concentrate hematopoietic progenitors. Blood *111*, 5298-5306. 10.1182/blood-2007-10-117622.
13. Nakamura, S., Sugimoto, N., and Eto, K. (2021). Development of platelet replacement therapy using human induced pluripotent stem cells. Dev Growth Differ *63*, 178-186. 10.1111/dgd.12711.

14. Flippe, L., Gaignerie, A., Serazin, C., Baron, O., Saulquin, X., Anegon, I., David, L., and Guillonneau, C. (2022). Generation of CD34(+)CD43(+) Hematopoietic Progenitors to Induce Thymocytes from Human Pluripotent Stem Cells. Cells *11*. 10.3390/cells11244046.
15. Wang, Y., Yates, F., Naveiras, O., Ernst, P., and Daley, G.Q. (2005). Embryonic stem cell-derived hematopoietic stem cells. Proc Natl Acad Sci U S A *102*, 19081-19086.
16. Narayan, A.D., Chase, J.L., Lewis, R.L., Tian, X., Kaufman, D.S., Thomson, J.A., and Zanjani, E.D. (2006). Human embryonic stem cell-derived hematopoietic cells are capable of engrafting primary as well as secondary fetal sheep recipients. Blood *107*, 2180-2183. 10.1182/blood-2005-05-1922.
17. Ledran, M.H., Krassowska, A., Armstrong, L., Dimmick, I., Renstrom, J., Lang, R., Yung, S., Santibanez-Coref, M., Dzierzak, E., Stojkovic, M., et al. (2008). Efficient hematopoietic differentiation of human embryonic stem cells on stromal cells derived from hematopoietic niches. Cell Stem Cell *3*, 85-98.
18. Risueno, R.M., Sachlos, E., Lee, J.H., Lee, J.B., Hong, S.H., Szabo, E., and Bhatia, M. (2012). Inability of human induced pluripotent stem cell-hematopoietic derivatives to downregulate microRNAs in vivo reveals a block in xenograft hematopoietic regeneration. Stem Cells *30*, 131-139. 10.1002/stem.1684.
19. Sandler, V.M., Lailler, N., and Bouhassira, E.E. (2011). Reprogramming of embryonic human fibroblasts into fetal hematopoietic progenitors by fusion with human fetal liver CD34+ cells. PLoS One *6*, e18265. 10.1371/journal.pone.0018265.
20. Szabo, E., Rampalli, S., Risueno, R.M., Schnerch, A., Mitchell, R., Fiebig-Comyn, A., Levadoux-Martin, M., and Bhatia, M. (2010). Direct conversion of human fibroblasts to multilineage blood progenitors. Nature *468*, 521-526. 10.1038/nature09591.
21. Sandler, V.M., Lis, R., Liu, Y., Kedem, A., James, D., Elemento, O., Butler, J.M., Scandura, J.M., and Rafii, S. (2014). Reprogramming human endothelial cells to haematopoietic cells requires vascular induction. Nature *511*, 312-318. 10.1038/nature13547.
22. Doulatov, S., Vo, L.T., Chou, S.S., Kim, P.G., Arora, N., Li, H., Hadland, B.K., Bernstein, I.D., Collins, J.J., Zon, L.I., and Daley, G.Q. (2013). Induction of multipotential hematopoietic progenitors from human pluripotent stem cells via respecification of lineage-restricted precursors. Cell Stem Cell *13*, 459-470. 10.1016/j.stem.2013.09.002.
23. Sugimura, R., Jha, D.K., Han, A., Soria-Valles, C., da Rocha, E.L., Lu, Y.F., Goettel, J.A., Serrao, E., Rowe, R.G., Malleshaiah, M., et al. (2017). Haematopoietic stem and progenitor cells from human pluripotent stem cells. Nature *545*, 432-438. 10.1038/nature22370.
24. Lis, R., Karrasch, C.C., Poulos, M.G., Kunar, B., Redmond, D., Duran, J.G.B., Badwe, C.R., Schachterle, W., Ginsberg, M., Xiang, J., et al. (2017). Conversion of adult endothelium to immunocompetent haematopoietic stem cells. Nature *545*, 439-445. 10.1038/nature22326.
25. Amabile, G., Welner, R.S., Nombela-Arrieta, C., D'Alise, A.M., Di Ruscio, A., Ebralidze, A.K., Kraytsberg, Y., Ye, M., Kocher, O., Neuberg, D.S., et al. (2013). In vivo generation of transplantable human hematopoietic cells from induced pluripotent stem cells. Blood *121*, 1255-1264. 10.1182/blood-2012-06-434407.
26. Suzuki, N., Yamazaki, S., Yamaguchi, T., Okabe, M., Masaki, H., Takaki, S., Otsu, M., and Nakauchi, H. (2013). Generation of engraftable hematopoietic stem cells from induced pluripotent stem cells by way of teratoma formation. Mol Ther *21*, 1424-1431. 10.1038/mt.2013.71.
27. McDonald, D., Wu, Y., Dailamy, A., Tat, J., Parekh, U., Zhao, D., Hu, M., Tipps, A., Zhang, K., and Mali, P. (2020). Defining the Teratoma as a Model for Multi-lineage Human Development. Cell *183*, 1402-1419 e1418. 10.1016/j.cell.2020.10.018.
28. Dzierzak, E., and Bigas, A. (2018). Blood Development: Hematopoietic Stem Cell Dependence and Independence. Cell Stem Cell *22*, 639-651. 10.1016/j.stem.2018.04.015.
29. Canu, G., and Ruhrberg, C. (2021). First blood: the endothelial origins of hematopoietic progenitors. Angiogenesis *24*, 199-211. 10.1007/s10456-021-09783-9.

30. Ottersbach, K. (2019). Endothelial-to-haematopoietic transition: an update on the process of making blood. Biochem Soc Trans *47*, 591-601. 10.1042/BST20180320.
31. Lange, L., Morgan, M., and Schambach, A. (2021). The hemogenic endothelium: a critical source for the generation of PSC-derived hematopoietic stem and progenitor cells. Cell Mol Life Sci *78*, 4143-4160. 10.1007/s00018-021-03777-y.
32. Sturgeon, C.M., Ditadi, A., Clarke, R.L., and Keller, G. (2013). Defining the path to hematopoietic stem cells. Nat Biotechnol *31*, 416-418. 10.1038/nbt.2571.
33. Slukvin, I. (2013). Hematopoietic specification from human pluripotent stem cells: current advances and challenges toward de novo generation of hematopoietic stem cells. Blood *122*, 4035-4046. 10.1182/blood-2013-07-474825.
34. Vo, L.T., and Daley, G.Q. (2015). De novo generation of HSCs from somatic and pluripotent stem cell sources. Blood *125*, 2641-2648. 10.1182/blood-2014-10-570234.
35. Arboretti, R., Ceccato, R., Pegoraro, L., Salmaso, L., Housmekerides, C., Spadoni, L., Pierangelo, E., Quaggia, S., Tveit, C., and Vianello, S. (2022). Machine learning and design of experiments with an application to product innovation in the chemical industry. J Appl Stat *49*, 2674-2699. 10.1080/02664763.2021.1907840.
36. Huang, S., and Terstappen, L.W. (1994). Lymphoid and myeloid differentiation of single human CD34+, HLA-DR+, CD38- hematopoietic stem cells. Blood *83*, 1515-1526.
37. Chadwick, K., Wang, L., Li, L., Menendez, P., Murdoch, B., Rouleau, A., and Bhatia, M. (2003). Cytokines and BMP-4 promote hematopoietic differentiation of human embryonic stem cells. Blood *102*, 906-915.
38. Lam, A.C., Li, K., Zhang, X.B., Li, C.K., Fok, T.F., Chang, A.M., James, A.E., Tsang, K.S., and Yuen, P.M. (2001). Preclinical ex vivo expansion of cord blood hematopoietic stem and progenitor cells: duration of culture; the media, serum supplements, and growth factors used; and engraftment in NOD/SCID mice. Transfusion *41*, 1567-1576. 10.1046/j.1537-2995.2001.41121567.x.
39. Vodyanik, M.A., Bork, J.A., Thomson, J.A., and Slukvin, II (2005). Human embryonic stem cell-derived CD34+ cells: efficient production in the coculture with OP9 stromal cells and analysis of lymphohematopoietic potential. Blood *105*, 617-626.
40. Lengerke, C., Grauer, M., Niebuhr, N.I., Riedt, T., Kanz, L., Park, I.H., and Daley, G.Q. (2009). Hematopoietic development from human induced pluripotent stem cells. Ann N Y Acad Sci *1176*, 219-227. 10.1111/j.1749-6632.2009.04606.x.
41. Watari, K., Lansdorp, P.M., Dragowska, W., Mayani, H., and Schrader, J.W. (1994). Expression of interleukin-1 beta gene in candidate human hematopoietic stem cells. Blood *84*, 36-43.
42. Ditadi, A., Sturgeon, C.M., Tober, J., Awong, G., Kennedy, M., Yzaguirre, A.D., Azzola, L., Ng, E.S., Stanley, E.G., French, D.L., et al. (2015). Human definitive haemogenic endothelium and arterial vascular endothelium represent distinct lineages. Nat Cell Biol *17*, 580-591. 10.1038/ncb3161.
43. Dick, J.E., Pflumio, F., and Lapidot, T. (1991). Mouse models for human hematopoiesis. Semin Immunol *3*, 367-378.
44. Tourino, C., Pflumio, F., Novault, S., Masse, A., Guiller, M., Bonnet, M.L., Valteau-Couanet, D., Hartmann, O., Vainchenker, W., Beaujean, F., et al. (2001). Efficient ex vivo expansion of NOD/SCID-repopulating cells with lympho-myeloid potential in hematopoietic grafts of children with solid tumors. Hematol J *2*, 108-116. 10.1038/sj/thj/6200083.
45. Vodyanik, M.A., Thomson, J.A., and Slukvin, II (2006). Leukosialin (CD43) defines hematopoietic progenitors in human embryonic stem cell differentiation cultures. Blood *108*, 2095-2105. 10.1182/blood-2006-02-003327.
46. Uenishi, G., Theisen, D., Lee, J.H., Kumar, A., Raymond, M., Vodyanik, M., Swanson, S., Stewart, R., Thomson, J., and Slukvin, I. (2014). Tenascin C promotes hematoendothelial development and T lymphoid commitment from human pluripotent stem cells in chemically defined conditions. Stem Cell Reports *3*, 1073-1084. 10.1016/j.stemcr.2014.09.014.

47. Audige, A., Rochat, M.A., Li, D., Ivic, S., Fahrny, A., Muller, C.K.S., Gers-Huber, G., Myburgh, R., Bredl, S., Schlaepfer, E., et al. (2017). Long-term leukocyte reconstitution in NSG mice transplanted with human cord blood hematopoietic stem and progenitor cells. BMC Immunol *18*, 28. 10.1186/s12865-017-0209-9.
48. Shultz, L.D., Lyons, B.L., Burzenski, L.M., Gott, B., Chen, X., Chaleff, S., Kotb, M., Gillies, S.D., King, M., Mangada, J., et al. (2005). Human lymphoid and myeloid cell development in NOD/LtSz-scid IL2R gamma null mice engrafted with mobilized human hemopoietic stem cells. J Immunol *174*, 6477-6489. 10.4049/jimmunol.174.10.6477.
49. Fulcher, D., and Wong, S. (1999). Carboxyfluorescein succinimidyl ester-based proliferative assays for assessment of T cell function in the diagnostic laboratory. Immunol Cell Biol *77*, 559-564. 10.1046/j.1440-1711.1999.00870.x.
50. Huang, X., Lee, M.R., Cooper, S., Hangoc, G., Hong, K.S., Chung, H.M., and Broxmeyer, H.E. (2016). Activation of OCT4 enhances ex vivo expansion of human cord blood hematopoietic stem and progenitor cells by regulating HOXB4 expression. Leukemia *30*, 144-153. 10.1038/leu.2015.189.
51. Crosse, E.I., Gordon-Keylock, S., Rybtsov, S., Binagui-Casas, A., Felchle, H., Nnadi, N.C., Kirschner, K., Chandra, T., Tamagno, S., Webb, D.J., et al. (2020). Multi-layered Spatial Transcriptomics Identify Secretory Factors Promoting Human Hematopoietic Stem Cell Development. Cell Stem Cell *27*, 822-839 e828. 10.1016/j.stem.2020.08.004.
52. Smadja, D.M., Cornet, A., Emmerich, J., Aiach, M., and Gaussem, P. (2007). Endothelial progenitor cells: characterization, in vitro expansion, and prospects for autologous cell therapy. Cell Biol Toxicol *23*, 223-239. 10.1007/s10565-007-0177-6.
53. Calvanese, V., Capellera-Garcia, S., Ma, F., Fares, I., Liebscher, S., Ng, E.S., Ekstrand, S., Aguade-Gorgorio, J., Vavilina, A., Lefaudeux, D., et al. (2022). Mapping human haematopoietic stem cells from haemogenic endothelium to birth. Nature. 10.1038/s41586-022-04571-x.
54. Zeng, Y., He, J., Bai, Z., Li, Z., Gong, Y., Liu, C., Ni, Y., Du, J., Ma, C., Bian, L., et al. (2019). Tracing the first hematopoietic stem cell generation in human embryo by single-cell RNA sequencing. Cell Res *29*, 881-894. 10.1038/s41422-019-0228-6.
55. Ivanovs, A., Rybtsov, S., Welch, L., Anderson, R.A., Turner, M.L., and Medvinsky, A. (2011). Highly potent human hematopoietic stem cells first emerge in the intraembryonic aorta-gonad-mesonephros region. J Exp Med *208*, 2417-2427. jem.20111688 [pii] 10.1084/jem.20111688.
56. Rongvaux, A., Takizawa, H., Strowig, T., Willinger, T., Eynon, E.E., Flavell, R.A., and Manz, M.G. (2013). Human hemato-lymphoid system mice: current use and future potential for medicine. Annu Rev Immunol *31*, 635-674. 10.1146/annurev-immunol-032712-095921.
57. Sippel, T.R., Radtke, S., Olsen, T.M., Kiem, H.P., and Rongvaux, A. (2019). Human hematopoietic stem cell maintenance and myeloid cell development in next-generation humanized mouse models. Blood Adv *3*, 268-274. 10.1182/bloodadvances.2018023887.
58. Ito, M., Hiramatsu, H., Kobayashi, K., Suzue, K., Kawahata, M., Hioki, K., Ueyama, Y., Koyanagi, Y., Sugamura, K., Tsuji, K., et al. (2002). NOD/SCID/gamma(c)(null) mouse: an excellent recipient mouse model for engraftment of human cells. Blood *100*, 3175-3182. 10.1182/blood-2001-12-0207.
59. Fitch, S.R., Kimber, G.M., Wilson, N.K., Parker, A., Mirshekar-Syahkal, B., Gottgens, B., Medvinsky, A., Dzierzak, E., and Ottersbach, K. (2012). Signaling from the sympathetic nervous system regulates hematopoietic stem cell emergence during embryogenesis. Cell Stem Cell *11*, 554-566. S1934-5909(12)00417-1 [pii] 10.1016/j.stem.2012.07.002.
60. Kobari, L., Pflumio, F., Giarratana, M., Li, X., Titeux, M., Izac, B., Leteurtre, F., Coulombel, L., and Douay, L. (2000). In vitro and in vivo evidence for the long-term multilineage (myeloid, B,

NK, and T) reconstitution capacity of ex vivo expanded human CD34(+) cord blood cells. Exp Hematol *28*, 1470-1480. 10.1016/s0301-472x(00)00557-9.

61. Hu, Y., and Smyth, G.K. (2009). ELDA: extreme limiting dilution analysis for comparing depleted and enriched populations in stem cell and other assays. J Immunol Methods *347*, 70-78. 10.1016/j.jim.2009.06.008.

62. Young, M.D., and Behjati, S. (2020). SoupX removes ambient RNA contamination from droplet-based single-cell RNA sequencing data. Gigascience *9*. 10.1093/gigascience/giaa151.

63. Han, X., Zhou, Z., Fei, L., Sun, H., Wang, R., Chen, Y., Chen, H., Wang, J., Tang, H., Ge, W., et al. (2020). Construction of a human cell landscape at single-cell level. Nature *581*, 303-309. 10.1038/s41586-020-2157-4.

64 Hao, Y., Hao, S., Andersen-Nissen, E., Mauck, W.M., 3rd, Zheng, S., Butler, A., Lee, M.J., Wilk, A.J., Darby, C., Zager, M., et al. (2021). Integrated analysis of multimodal single-cell data. Cell *184*, 3573-3587 e3529. 10.1016/j.cell.2021.04.048.

FIGURE LEGENDS

Figure 1: Design of Experiment step by step.

Based on a literature review (see references in Table S1), an ensemble of cytokines and growth factors was identified (input variables) and a range of input concentrations was defined for each of them. Output variables such as cell surface markers (Table S2), cell proliferation, and LTC-IC frequency were defined. Based on these variables, 16 experimental designs were created that differed in their individual concentrations of growth factors and cytokines (Table S1). Baseline variable data from the 16 different experimental designs were collected. Based on these results, mathematical modeling of the interactions between the input and output variables was calculated. Three final combinations were proposed and tested, first with flow cytometry analysis on two different hiPSC lines (ie, FD136-25 and IMR90-16) (n=1 and n=1 independent experiments respectively) and second with mouse transplants using the FD136-25 line (n=15, 2 independent experiments). Statistical data are presented as box plots and are mean ± SD or SEM according to the number of independent experiments. Wilcoxon Mann-Whitney test.

See also supplemental experimental procedures and Tables S1, S2, and S3.

Figure 2: *In vivo* primary engraftment of D17 EB cells in immunocompromised NSG mice.

(A) hiPSCs (5 different cell lines) were differentiated in liquid culture supplemented with combination A of growth factors and cytokines for a total period of 17 days. EB or $CD34^+$ CB cells (4.10^5) were dissociated and inoculated into irradiated primary NSG recipients over a total period of 20 weeks. BM cells from primary recipients were collected and inoculated into secondary irradiated NSG recipients (7.10^6 cells) over a further period of 20 weeks.

(B) Flow cytometric analysis of human and mouse $CD45^+$ cell expression in BM of a representative primary recipient.

(C) Multilineage analysis by FACS on NSG mice BM, 20 weeks post-transplantation, on $hCD34^+hCD43^+$ and $hCD45^+$ HSPCs into primary recipients. All mixed hiPSC lines. Each circle/square/triangle represents a single animal. n=59, 14 independent experiments.

(D) Multilineage analysis from the five individual hiPSC lines: FD136-25 (n= 10 mice, 3 independent experiments, red circles), PC1429 (n=10, 3 independent experiments, orange

squares), PCi-CAU (n= 26, 4 independent experiments, green triangles), LAM001.005 (n=6, 2 independent experiments, light blue lozenges) and LAM002.002 (n=7, 2 independent experiments, dark blue lozenges) and the $CD34^+$ CB cells (n=13, 3 independent experiments, grey circles) in NSG primary recipients 20 weeks after transplantation of $4x10^5$ D17 EB or $CD34^+$ CB cells. FACS results are expressed as % of $hCD34^+$, $hCD43^+$, and $hCD45^+$. The results are relatively equivalent between the lines and close to the CD34 control. The dotted line indicates the limit of 0.1% of $hCD45^+$ usually considered positive for human hematopoietic transplantation in NSG mice [43].

(E) Distribution of human myeloid, B-lymphoid, and T-lymphoid cells ($hCD33^+$, $hCD19^+$, and $hCD3^+$, respectively) and $hCD235a^+$ erythroid progenitors/precursors in the grafted BM 20 weeks after transplantation of each of the five hiPSCs lines compared with $CD34^+$ CB cells. Same number of animals and presentation as in (D).

(F) Flow cytometric analysis of a representative animal for myeloid (hCD14/hCD15), lymphoid (hCD19/hIgM, SSC-A/hCD3) and pro-erythroid (hCD71/hCD235a) lineages in the grafted BM. Myeloid and lymphoid cells are analyzed from $hCD45^+$ gated BM cells whereas hCD71/hCD235a (Pro-E) was analyzed on whole BM cells.

(G) Flow cytometric analysis of a representative animal for the distribution of hCD3, hCD4 and hCD8 antigens and of hTCRαβ and γδ in T lymphoid cells in a grafted thymus.

(H) Distribution of T, B, Pro-erythrocyte and monocyte lineages in representative individual primary recipients analyzed by flow cytometry. Mice 1-6, a-e and L1-L5 are from one independent experiment analyzed at one week interval i.e., a-e and L1-L5 were analyzed at the same time by two independent laboratories.

Statistical data are presented as box plots and are mean ± SEM. Wilcoxon Mann-Whitney test.

Figure 3: Single cell transcriptome and phenotypic analysis of the grafted NSG BM.

(A, B) UMAP embedding of a merged data set from two representative transplanted mice (mice L1 and L5, displayed in Figure 2H). BM data set colored by cell type (A) and by sample (B).

(C) UMAP embedding of a merged dataset of human cells in the two engrafted BM datasets colored by cell type.

(D) UMAP representation of single-cell RNA-Seq from NSG mouse L5 BM (14173 cells) transplanted with D17 EB cells for 20 weeks. Mouse and human cell clusters are identified.

(E-F) Bone marrow of NSG mouse L5 primary recipient analyzed by FACS at 20 weeks for (E) human erythroid cells (hCD235a$^+$ and hCD235a+hCD71$^+$) and (F) B cells (hIgM$^+$CD10$^+$), neutrophils (hCD33$^+$hCD14$^+$), and T cells (hCD4$^+$hCD3$^+$).

(G) Expression of globin genes in human early erythroid cells in transplanted mouse bone marrow datasets.

Figure 4: **Functional assessment of the grafted cells**

(A) Clonogenic hematopoietic assays on BM cells isolated from primary recipients grafted with either D17 EB (n=59, 14 independent experiments) or CD34$^+$ CB cells (n=13, 3 independent experiments). Frequency of CFU-GM, BFU-E, and CFU-GEMM colonies.

(B) Representative colonies of CFU-GEMM (1), CFU-E (2) and CFU-GM (3) from D17 EB primary BM cells (n=59, 14 independent experiments).

(C) Cytospins. May Grünwald-Giemsa staining of cells isolated from clonogenic assays in primary or secondary recipients. Mature macrophages (1), histio monocytes (2), myelocytes (2), and erythroblasts (3). B: bar=50µm; C: bar= 10µm

(D) Human globin expression from CB CD34$^+$HSPCs erythroid culture (n=3), from BM primary (n=12) and secondary recipients (n=4) and pooled BFU-E from BM primary recipients (6 to 10 BFU-E pooled. n=12, 3 independent experiments. Data are mean ± SEM

(E) Maturation of human T cells. Peripheral blood from a representative grafted primary recipient stained with antibodies against hTCR αβ and hTCR γδ. Cells are first gated for hCD3 and analyzed for TCR expression.

(F) Representative example of Human T cell amplification under hCD3 and hCD23 stimulation. The entire thymic population is labeled with CFSE at D0. During 5 days the labeled cells were cultured with or without hCD3 and hCD23. At D5, the unstimulated population is red, while the stimulated parent population is blue and the D0 population is green (n=6, 3 independent experiments).

(G) Confidence intervals of 1/(stem cell frequency) were calculated by ELDA (http://bioinf.wehi.edu.au/software/elda/) according to the Poisson distribution.

Statistical data are presented as box plots and are mean ± SEM. Wilcoxon Mann-Whitney test.

Figure 5: *In vivo* engraftment of D17 EB cells in immunocompromised NSG mice, secondary recipients.

(A) Flow cytometric analysis of human and mouse $CD45^+$ cell expression in BM of a representative secondary recipient.

(B) *In vivo* engraftment of D17 human EB cells. All mixed hiPSC lines. Each circle/square/triangle represents a single animal. n= 40, 10 independent experiments.

(C) *In vivo* engraftment of D17 human EB cells from the five individual hiPSC lines: FD136-25 (n=10, 3 independent experiments, red circles), PC1429 (n=10, 3 independent experiments, orange squares), PCi-CAU (n=10, 3 independent experiments, green triangles), LAM001.005 (n=4, 2 independent experiments, light blue lozenges) and LAM002.002 (n=6, 2 independent experiments, dark blue lozenges) and the $CD34^+$ CB cells (n=13, 3 independent experiments, grey circles) in NSG secondary recipients 20 weeks after transplantation of 7.10^6 BM cells. FACS results are expressed as % of $hCD34^+$, $hCD43^+$, and $hCD45^+$.

(D) Multilineage analysis. Human myeloid, B-lymphoid, and T-lymphoid cells ($hCD33^+$, $hCD19^+$, and $hCD3^+$, respectively) and $hCD235a^+$ erythroid progenitors/precursors 20 weeks after transplantation of the bone marrow from primary mice that received each of the five D17 EB cells compared with $CD34^+$ CB cells. Same number of animals and presentation as in (C).

(E) Flow cytometric analysis of a representative secondary recipient transplanted with 7.10^6 D17 EB cells. Myeloid (hCD33), B lymphoid (hCD19), T lymphoid (hCD3) and pro-erythroid (hCD71/hCD235a) lineages. Myeloid and lymphoid cells are analyzed from $hCD45^+$ gated BM cells whereas Pro-E hCD71/hCD235a was analyzed on whole BM cells.

(F) Clonogenic hematopoietic assays on BM cells isolated from secondary recipients grafted with either D17 EB (n=10, 2 independent experiments) or $CD34^+$ CB cells (n=13, 3 independent experiments). Frequency of CFU-GM, BFU-E, and CFU-GEMM colonies.

Statistical data are presented as box plots and are mean ± SEM. Wilcoxon Mann-Whitney test.

Figure 6: Transcriptomic analysis of the EB cells

(A) UMAP embeddings of cells in EBs at D13, 15, 17, and 19, 26027 cells. EVT : Extravillous

Trophoblast. MEP: Megakaryocyte-Erythroid Progenitors. ECM: Extracellular Matrix. AGM: Aorta-Gonad-Mesonephros.

(B) Expression of genes in Crosse et al., 2020 characterizing endothelial populations in the AGM applied to the EB dataset

(C) UMAP embedding of cells in the data set of Crosse et al., 2020. HSPC : Hematopoietic stem and progenitor cells. PGC: Primordial germ cells. Hem: Hematopoietic cells. CL8: Cluster 8 described in Crosse et al., 2020 [50].

(D) Expression of genes described in Crosse et al., 2020 [50] characterizing endothelial populations in the AGM applied to Crosse et al. data set.

(E) Close-up of the UMAP embedding on the hematopoietic cell populations in the EB dataset framed in A. MEP: Megakaryocyte-Erythroid Progenitors. HSC: Hematopoietic Stem Cells. HE: Hemogenic Endothelium. Erythro: Erythroid cells.

(F) Expression of the six-gene molecular HSC signature of Calvanese et al., 2022 [52] in the hematopoietic population of the embryoid body dataset.

Figure 7: Molecular characterization of the cells in the embryoid bodies

(A-C) Time-course detection of molecular markers of endothelial and hematopoietic cell populations between scRNA-Seq and q-PCR datasets comparison (A), in FACS (B) and scRNA-Seq (C).

(D-G) Immunostaining on transverse sections of D17 EBs showing spatial organization of endothelium and peri-endothelial populations. (D) Endothelial cells (CDH5). (E, F) cells expressing PECAM1 and the transcription factor RUNX1. (G) Pericytes ($NG2^+$) and smooth muscle cells (αSMA^+).

D, E, F, G: Bars=100 microns.

- **Please include these specific headings in the following order: RESOURCE AVAILABILITY; EXPERIMENTAL MODEL AND SUBJECT DETAILS; METHOD DETAILS; QUANTIFICATION AND STATISTICAL ANALYSIS and add all the relevant information, as further explained in the attached document.**

STAR★Methods

RESOURCE AVAILABILITY

Lead contact

Requests for further information should be directed to and will be fulfilled by the lead contact, Laurence Guyonneau-Harmand (laurence.harmand@upmc.fr).

Materials availability

This study did not generate any unique reagents.

Data and code availability

- Single-cell RNA-seq data have been deposited at the National Center for Biotechnology Information BioProjects Gene Expression Omnibus (GEO) under accession number GEO:GSE151877. Accession numbers are listed in the key resource table.
- *In vivo* single-cell RNAseq data from the human embryo were from Calvanese et al., [53] and Zeng et al. [54]
- No original code is reported in this paper.
- Any additional information required for re-analysis of the data reported in this paper is available on request from the lead contact.

EXPERIMENTAL MODEL AND PARTICIPANT DETAILS

Ethics statement

All experiments and procedures were performed in compliance with the French Ministry of Agriculture regulations for animal experimentation and approved by the local ethics committee (APAFIS approval number # 17559-2018111613396032v2 (2024)).

Animals

Two animal models were used for this study:

- NOD/SCID-LtSz-scid/scid (NOD/SCID) (Charles River, L'Abresle, France)
- NOD.Cg-Prkdc^{scid}Il2rg^{tm1Wjl}/SzJ or NSG (Charles River, L'Abresle, France)

We choose to work with female mice because they are less aggressive and this is an important factor when the experience lasts 20 weeks with regular sampling.

Cell lines

For cell lines, primary cultures, and microbe strains, please describe culture/growth conditions, including temperature. Sex of cells must also be reported

MS-5 [Mouse bone marrow] (RRID:CVCL_2128): mouse male cells are maintained in 90% alpha-MEM with ribo- and deoxyribonucleosides + 10% decomplemented FBS + 2 mM L-glutamine + 2 mM sodium pyruvate at 37°C and 5% CO_2 .

PCi-CAU : human male induced pluripotent stem cells are maintained on Matrigel™ (Corning) in mTESRplus medium (Stemcell Technologies) at 37°C and 5% CO_2 .

PCi-1429 : human female induced pluripotent stem cells are maintained on Matrigel™ (Corning) in mTESRplus medium (Stemcell Technologies) at 37°C and 5% CO_2 .

IMR90-16 : human female induced pluripotent stem cells are maintained on Matrigel™ (Corning) in mTESRplus medium (Stemcell Technologies) at 37°C and 5% CO_2 .

FD136-25 : human female induced pluripotent stem cells are maintained on Matrigel™ (Corning) in mTESRplus medium (Stemcell Technologies) at 37°C and 5% CO_2 .

LAM001.005 : human female induced pluripotent stem cells are maintained on Matrigel™ (Corning) in mTESRplus medium (Stemcell Technologies) at 37°C and 5% CO_2 .

LAM002.002 human male induced pluripotent stem cells are maintained on Matrigel™ (Corning) in mTESRplus medium (Stemcell Technologies) at 37°C and 5% CO_2 .

Cord blood $CD34^+$: We obtain cord blood units from AP-HP, Hôpital Saint-Louis, Unité de Thérapie cellulaire, CRB-Banque de Sang de Cordon, Paris, France(n° d'autorisation : AC-2016-2759) for research purposes only. They are therefore anonymized and the sex of the baby is not mentioned. $CD34^+$ are sorted and transplanted or seeded in methylcellulose with BSA, IMDM and SCF, IL-3, EPO and GM-CSF.

METHOD DETAILS

hiPSC amplification

The study was conducted using six different hiPSC lines: the FD136-25 (skin primary fibroblasts) reprogrammed with lentiviral vectors and Thomson's combination (endogenous expression of Oct4, Sox2, Nanog and Lin28), IMR90-16 (fetal lung fibroblasts) reprogrammed with lentiviral vectors and Thomson's combination (endogenous expression of Oct4, Sox2, Nanog and Lin28) [2], the Pci-1429 and Pci-CAU lines (peripheral blood mononuclear cells-Phenocell) reprogrammed with episomes (Sox2, Oct4, KLF, cMyc); the LAM001-005 and LAM002-002 lines (skin primary fibroblasts), reprogrammed with sendaï virus (Oct3/4, Nanog, KLF and cMyc) by IPS CDTC core facility, Nantes, France. hiPSCs were maintained on Matrigel™ (Corning) in mTESRplus medium (Stemcell Technologies) and the cells were passaged 1:6 onto freshly coated plates every 3 to 5 days using standard clump passaging with TRYple select (Invitrogen) or ReLeSR (Stemcell Technologies).

ABG ATMP platform worked with Pci-CAU line and used vitronectin matrix (Gibco™), IPSbrew medium (Miltenyi Biotec) and ReLeSR (Stemcell Technologies) for passaging.

Design of experiment

EBs were cultured in liquid medium IMDM supplemented with stabilized glutamine (SAFC), 330 µg/mL holo-human transferrin (Scipac), 10 µg/mL recombinant human insulin (Incelligent SG; CellGen), 2 IU/mL heparin Choay, and 5% solvent/detergent virus-inactivated AB plasma (Etablissement Français du Sang). This plasma is used in a clinical trial registered at http://www.clinicaltrials.gov as NCT0929266. Plasma samples can be obtained upon reasonable request.

Optimal response surface modeling was applied to determine the optimal concentrations of the 10 selected cytokines. A two-factorial experimental design was chosen with a range of 10 independent variables. The following cytokines were selected on the basis of personal experience and data from the literature: SCF (20 to 300 ng/mL), IGF-1 (5 to 50 ng/mL), TPO (20 to 100 ng/mL), IL1 (5 to 50 ng/mL), IL3 (5 to 50 ng/mL), IL6 (5 to 50 ng/mL), G-CSF (10 to 100 ng/mL), BMP4 (20 to 200 ng/mL), VEGF (20 to 200 ng/mL) and FLT3 (20 to 300 ng/mL) (Table S1). Human iPSCs were cultured for 17 days using 16 different combinations of cytokines. In each case, the cells were phenotyped and their amplification rate and their ability to generate LTC-ICs were determined (table S1). Statistical design, regression analysis of the results and plotting of the response surface were performed using the software JMP-8 (SAS Institute Inc., Cary, USA). The software generated an algorithm which identified three efficient combinations of cytokines (table S2).

EB differentiation

The EB culture medium (see above) was supplemented with stem cell factor (24 ng/mL), thrombopoietin (21 ng/mL), FLT3 ligand (21 ng/mL), recombinant human bone morphogenetic protein 4 (194 ng/mL), recombinant human vascular endothelial growth factor (200 ng/mL), interleukin-3 (50 ng/mL), interleukin-6 (50 ng/mL), interleukin-1 (5 ng/mL), granulocyte colony-stimulating factor (100 ng/mL) and insulin growth factor (1 ng/mL) (GMP grade when available otherwise Premium grade, Peprotech) . The medium was replenished every other day until 19 days at 37°C in a humidified 5% CO_2 atmosphere. EBs were dissociated in 0.1% collagenase B (Roche Diagnostics, Laval, QC, Canada) for 1 hour at 37°C then 0.25% trypsin for 3 min and disrupted by gentle mechanical agitation

Colony assays

At the indicated times, 10^5 dissociated EB cells or 3.10^4 cells from xenotransplanted recipient BM were plated into 3 mL of complete methylcellulose medium in the presence of SCF, IL-3, EPO and GM-CSF (PeproTech, Neuilly-sur-Seine, France). As G-CSF also stimulates mouse progenitors, it was replaced by granulocyte-macrophage colony-stimulating factor (GM-CSF). Aliquots (1 mL) of the mix were distributed into one 30 mm dish twice and maintained in a humidified chamber for 14 days. Colony-forming Cells (CFC) were scored on day 14.

Long-term culture-initiating cell assay

Long-term culture-initiating cell (LTC-IC) assays were performed as described previously [60], 15–100,000 cells/well on day 17 for the EBs and on day 0 for the control $CD34^+$. Absolute LTC-IC counts corresponded to the cell concentrations, yielding 37% negative wells using Poisson statistics.

Pseudo-microtubules

Growth factor-reduced Matrigel (Becton Dickinson, New Jersey, USA) was thawed, placed in 24-well plates, and allowed to stand at 37°C for 30 minutes to solidify. Aliquots of $5x10^4$ hiPSC cells/well were plated in 1 ml EBF2 medium (Lonza, Walkersville, USA) and incubated at 37°C for one week. A tubule is defined as a structure whose length is four times its width. The presence of tubules was checked daily, and they usually form within the first 6 hours.

Flow cytometry

Staining of hiPSCs or dissociated EBs or mouse tissue cells was performed with $2\text{-}5.10^5$cells in 100 µL staining buffer (PBS containing 2% FBS and FcR Blocking Reagent) with 5:100 dilution of each antibody, for 20 min at room temperature in the dark. Viability staining was performed using either DAPI or the Zombie aqua fixable viability kit (Biolegend). Data were collected using a Becton Dickinson Canto II cytometer or a MACS Quant VyB or a MACS Quant 10 (Miltenyi).

Three labs analyzed the data, the list of antibodies is given in “Key ressources methods”.

Real-Time Quantitative PCR

After isolation of total mRNA with an RNA minikit (Qiagen, Courtaboeuf, France), the mRNA integrity was checked by analysis on a Bioanalyzer 2100 (Agilent Technologies, Massy, France).

Complementary DNAs were constructed by reverse transcription with Superscript (Life Technologies, Carlsbad, USA). PCR assays were performed using a TaqMan PCR master mix (Life Technologies) and specific primers (Applied BioSystems, Carlsbad, USA) for selected genes (see table below), together with a sequence detection system (QuantStudio™ 12K Flex Real-Time PCR System, Life Technologies). In each sample the fluorescent PCR signal of each target gene was normalized to the fluorescent signal of the housekeeping gene glyceraldehyde 3-phosphate dehydrogenase (GAPDH).

Mouse transplantation

NOD/SCID-LtSz-scid/scid (NOD/SCID) and NOD.Cg-Prkdc^{scid}Il2rg^{tm1Wjl}/SzJ (NSG) (Charles River, L'Abresle, France) were housed in the IRSN animal care facility. All experiments and procedures were performed in compliance with the French Ministry of Agriculture regulations for animal experimentation and approved by

the local ethics committee (APAFIS approval number # 17559-2018111613396032v2 (2024)).

Mice, 5-8 weeks old and raised under sterile conditions, were sublethally irradiated with 2.4-3.5 Grays from a 137Cs source (2.115 Gy/min) 24 h before cell injection. To ensure consistency between experiments, only male mice were used. Prior to transplantation, the mice were temporarily sedated with an intraperitoneal injection of ketamine and xylazine. In primary recipients, 4 x10^5 D17 or CD34$^+$ CB cells (cord blood obtained from AP-HP, Hôpital Saint-Louis, Unité de Thérapie Cellulaire, CRB-Banque de Sang de Cordon, Paris, France (authorization number : AC-2016-2759) per mouse were transplanted by retro-orbital injection in a volume of 100 µl with a 28.5-gauge insulin needle. Secondary recipients were transplanted with 7,10^6 BM cells under the same conditions as the primary mice. A total of 251 mice were used in this study.

For the engraftment potential of the D17 cells on the five different hiPSC lines:

205 NSG mice were used as follows: 113 primary recipients, 53 secondary recipients and 39 as negative controls.

63 NOD-SCID mice were used as follows: 35 primary recipients and 16 secondary recipients, 3 tertiary recipients and 9 as negative controls (see Table S3). 4.10^5, 7.10^6 and 7.10^6 cells were inoculated for primary, secondary and tertiary recipients respectively.

Animals were analyzed 20 weeks after primary, secondary and even tertiary transplantation, with the exception of those processed on the ATM platform. These were analyzed after 8 and 12 weeks.

Limiting dilution.

For the limiting dilution assay (LDA), 33 NSG mice were used, i.e., 30 primary recipients and 3 controls. The number of human HSCs was determined by LDA. Increasing doses of d17 cells (1000, 5000, 10000, 50000, 100000) were retro-orbitally injected into sublethally irradiated NSG recipient mice. Twenty weeks after transplantation, the percentage of $hCD45^+$ cells were analyzed by flow cytometry. HSC frequency was calculated and recorded using ELDA software [61] (bioinf.wehi.edu.au/software/elda/).

Assessment of human cell engraftment

Most of the mice were sacrificed at week 20. A few of them were sacrificed at 8 or 12 weeks. Femurs, tibias, blood, liver, spleen and thymus were removed. Single cell suspensions were prepared by standard flushing and aliquots containing 7.10^5 cells were stained in a total volume of 100µL staining buffer (see also "Flow cytometry"). Non-injected mouse BM was used as a control for non-specific staining.

Data were acquired on a BD Canto II cytometer (Beckton Dinkinson), MACSQuant 10 and MACSQuant VYB (Miltenyi).

T-cell maturity and functionality assay

The presence of TCR αβ and TCR γδ in peripheral blood was assessed by flow cytometry using the following human markers: hCD3 clone UCHT1 (positive gating), TCR αβ clone IP26A and TCR γδ clone IMMU510 (all from Beckman Coulter antibodies, Brea, USA).

Thymus and spleen cells were isolated, CFSE labeled (cell trace CFSE cell proliferation kit, Thermofisher Scientific) and seeded in cell culture media complemented or not with hCD3 and

hCD28 (Beckman Coulter both 1mg/ml). After 5 days, cells were harvested and stained with anti-hCD3 clone UCHT1 and analyzed on a BD Canto II cytometer. FlowJo analysis software was used to gate on $CD3^{+}$T-cells and generate the overlaid histogram plots.

Cell preparation for sequencing

PCi-CAU EB cell suspensions at different times were loaded on a Chromium single cell instrument (10x Genomics, Pleasanton, CA, USA) to generate single-cell GEMs and prepared librairies according to the manufacturer's recommendations and performed Illumina Sequencing. Experiments were done in duplicates.

ScRNA-Seq analysis of mouse bone marrow

Both samples were aligned to mm10 and grch38 using CellRanger 6.1.2. For each sample, we selected only the cells expressing at least 200 genes in both genome assemblies. We identified the mouse cells from the human cells as described in the section "Separation strategy for human and mouse cells in scRNA-Seq" and filtered out the duplicates. Cells expressing less than 5000 genes on grch38 and 6000 genes on mm10 were retained. Cells expressing more than 10% of human mitochondrial RNA or 4% of mouse mitochondrial RNA were filtered out. The merged dataset from the two mice was then normalized using SCTransform with default parameters. UMAP visualization (n.neighbors=100) and Louvain clustering at 0.6 resolution were then performed for the first 38 PCA components. The same process was used for the mouse L5 and human cell plots, except for the number of PCA components selected, which varied: 39 for mouse L5 and 40 for human cells. Cell type identification was performed for the merged dataset of the two bone marrow cells with differentially expressed genes using SoupX tf-idf gene lists, scHCL and scMCA mapping, and manual examination of marker genes.

Separation strategy for human and mouse cells in BM scRNA-Seq

As a control, the human (SRR7881423) and mouse (SRR6835854) public BM datasets were aligned to mm10 and grch38 using CellRanger 6.0.0. Only cells that met CellRanger's filter threshold and had at least 200 features in grch38 or mm10 were selected for further analysis. All cells were then pooled and analyzed using the standard Seurat SCTransform pipeline for

grch38 data: SCTransform (default parameters), RunPCA, RunUMAP (first 40 PCA dimensions, n.neighbors=100).

As shown in Figure S2E, F, the ratio between the number of features detected in grch38 and mm10 assemblies was sufficient to clearly distinguish all human cells from mouse cells. In addition, the human and mouse datasets are separated in the final UMAP plot (Figure S2I).
In the mouse transplanted bone marrow dataset, although two populations could be separated based on the feature ratio of grch38/mm10, some cells had an intermediate ratio (Figure S2G, H). Because no cell type in the control exhibited such a phenotype and these intermediate cells were scattered across the different UMAP populations (Figure S2J), we considered them duplicates and filtered them out, resulting in the plot shown in Figure S2K. The human cells were those that had a ratio greater than 2.5 for mouse L1 and 2.85 for mouse L5. The mouse cells were those that had a ratio of less than 0.55 for mouse L1 and 0.47 for mouse L5. The total number of cells filtered (8%) was consistent with the expected number of duplicates using 10X Chromium technology.

ScRNA-Seq analysis of the embryoid bodies

Each individual sample was filtered to obtain only genes expressed in at least 3 cells and cells that expressed between 200 and 8000 genes. Due to a higher percentage of dead cells, only cells with more than 1300 genes were selected for one of the D15 datasets (J15-TJ3). Cells expressing more than 10% mitochondrial RNA were filtered out. The merged dataset was then normalized using SCTransform with default parameters. UMAP visualization and Leiden clustering with a resolution of 1.2 were then performed for the first 82 PCA components, the latter generated with the parameter approx= FALSE in Seurat. To identify cell type, differentially expressed genes were used with the Wilcoxon assay of Seurat, the tf-idf of SoupX, and the scHCL in addition to manual examination of marker genes to confirm cell identity.
To more accurately identify the cell type of hematopoietic cells, cells with a UMAP_1 coordinate less than -7 and a UMAP_2 coordinate greater than -1 were extracted and renormalized using SCTransform with default parameters. Leiden clustering was then performed at a resolution of 1.3 on the first 35 PCA dimensions. Cell type identification followed the same procedure as described for the entire dataset.

Immunostaining of the embryoid bodies

For immunofluorescence analysis (IF), EBs were fixed with 3.7% paraformaldehyde for 15 minutes at room temperature and sectioned using a Leica cryostat CM3050. Samples were then incubated for 60 minutes at room temperature with IF buffer [phosphate-buffered saline (PBS), 0.2% Triton, 5% FBS], which also served as a blocking solution. Samples were incubated with the primary antibodies overnight at 4 °C. The following antibodies were used: anti-alpha SMA (1:500; Sigma-Aldrich A2547), anti-NG2 (1:400, Cell Signaling E3B3G), anti-VECAD (1:400, Cell Signaling D87F2), anti-CD31 (1:500, Cell Signaling 89C2) and anti-RUNX1 (1:100, Abcamab 92336). Incubation with the secondary antibodies (1:500, Invitrogen A-21121, Jackson 711-605-152) was performed for 1 hour at room temperature. Finally, 40,6-diamidino-2-phenylindole (DAPI) nuclear staining was performed (1:500 for 5 minutes). Immunofluorescence images were acquired using a Leica DMi 6000B microscope. Images were processed using ImageJ software.

QUANTIFICATION AND STATISTICAL ANALYSIS

JMP-8 (SAS Institute Inc., Cary, USA) was used for DOE; the procedure is fully described in the Star Method above.

Confidence intervals of “LTC-IC frequency” and confidence intervals of “cell capable of graft frequency” were calculated using ELDA (http://bioinf.wehi.edu.au/software/elda/) according to Poisson distribution.

Graft quantification procedures are described in the Star Method. Criteria for successful engraftment were defined as >0.1% $hCD45^+$ cells in mouse BM. In the figure legend, we define “n” as the number of individual mice and indicate the number of biological replicates.

We did not exclude any animals.

In the text, we have chosen to present means +/- SEM, while in the figures we have chosen to present box plots, which are useful for visualizing the distribution of the data across its quartiles.

The list and versions of softwares, patches used for scRNA-Seq analysis will be provided upon request.

Statistical analyses were performed using GraphPad Prism 8 and Excel.

KEY RESOURCES TABLE

REAGENT or RESOURCE	SOURCE	IDENTIFIER
Antibodies		
Mouse IgG1 anti hCD90-FITC	**Beckman Coulter antibodies (Brea, USA)**	IM1893U
Mouse IgG1 anti hCD109-PE	**Beckman Coulter antibodies (Brea, USA)**	A08933
Mouse IgG1 anti hCD34-PE	**Beckman Coulter antibodies (Brea, USA)**	IM2648U
Mouse IgG1 anti hCD34-APC	**Beckman Coulter antibodies (Brea, USA)**	IM2472
Mouse IgG1 anti hCD117-PC5.5	**Beckman Coulter antibodies (Brea, USA)**	A66333
Mouse IgG1 anti hCD38-PC7	**Beckman Coulter antibodies (Brea, USA)**	A54189
Mouse IgG1 anti hCD3-FITC	**Beckman Coulter antibodies (Brea, USA)**	A07747
Mouse IgG1 anti hCD4-FITC	**Beckman Coulter antibodies (Brea, USA)**	A07750
Mouse IgG1 anti hCD8-PE	**Beckman Coulter antibodies (Brea, USA)**	A07757
Mouse IgG1 anti hCD19-FITC	**Beckman Coulter antibodies (Brea, USA)**	A07768
Mouse IgG1 anti hIgM-FITC	**Beckman Coulter antibodies (Brea, USA)**	B30655
Mouse IgG1 anti hTCR αβ-PE	**Beckman Coulter antibodies (Brea, USA)**	B49177
Mouse IgG1 anti hTCR γδ-FITC	**Beckman Coulter antibodies (Brea, USA)**	IM1571U
Mouse IgG1 anti hCD43-FITC	**Beckman Coulter antibodies (Brea, USA)**	IM3264U
Mouse IgG1 anti hCD43-PE	**Beckman Coulter antibodies (Brea, USA)**	A32560
Mouse IgG1 anti hCD45-KRO	**Beckman Coulter antibodies (Brea, USA)**	A96416
Mouse IgG1 anti hCD45-PC5.5	**Beckman Coulter antibodies (Brea, USA)**	A62835
Mouse IgG1 anti hCD14-FITC	**Beckman Coulter antibodies (Brea, USA)**	IM0645U
Mouse IgG1 anti hCD33 APC-A750	**Beckman Coulter antibodies (Brea, USA)**	A70200
Mouse IgG1 anti hCD15-PE	**Beckman Coulter antibodies (Brea, USA)**	IM1954U
Mouse IgG1 anti hCD13-ECD	**Beckman Coulter antibodies (Brea, USA)**	A33097

Mouse IgG1 anti hCD235a-FITC	**Beckman Coulter antibodies (Brea, USA)**	IM2212
Mouse IgG1 anti hCD71-APC-A750	**Beckman Coulter antibodies (Brea, USA)**	A89313
Mouse IgG1 anti hCD146-PE	**Beckman Coulter antibodies (Brea, USA)**	A07483
Mouse IgG1 anti hCD309-PE	**Beckman Coulter antibodies (Brea, USA)**	A64615
Mouse IgG1 anti hCD31-PE	**Beckman Coulter antibodies (Brea, USA)**	IM02409
Mouse IgG1 anti h HLA-DR-PB	**Beckman Coulter antibodies (Brea, USA)**	A74781
Mouse IgG1 anti FITC	**Beckman Coulter antibodies (Brea, USA)**	A07795
Mouse IgG1 anti PE	**Beckman Coulter antibodies (Brea, USA)**	A07796
Mouse IgG1 Mouse anti ECD	**Beckman Coulter antibodies (Brea, USA)**	A07797
Mouse IgG1 anti PC5.5	**Beckman Coulter antibodies (Brea, USA)**	A62833
Mouse IgG1 anti PC7	**Beckman Coulter antibodies (Brea, USA)**	737662
Mouse IgG1anti PB	**Beckman Coulter antibodies (Brea, USA)**	A74764
Mouse IgG1 anti APC A750	**Beckman Coulter antibodies (Brea, USA)**	A79393
Mouse IgG1 anti APC	**Beckman Coulter antibodies (Brea, USA)**	IM2475
monoclonal mouse anti-alpha SMA	Sigma-Aldrich	A2547
monoclonal rabbit anti-NG2	Cell Signaling Technology	E3B3G
monoclonal rabbit anti-VECAD	Cell Signaling Technology	D87F2
monoclonal mouse anti-CD31	Cell Signaling Technology	89C2
monoclonal rabbit anti-RUNX1 .	Abcam	92336
Goat anti-Mouse IgG1 Cross-Adsorbed, Alexa Fluor™488	Invitrogen	A-21121
Alexa Fluor® 647-AffiniPure	Jackson	711-605-152

Donkey Anti-Rabbit IgG (H+L)		
DAPI	Cell Signaling Technology	8961
Mouse IgG1 hCD3	Beckman Coulter	IM1280
Mouse IgG1 hCD28	Beckman Coulter	IM1376
Mouse IgGM anti SSEA1-FITC	BD Biosciences	560127
Mouse IgG3, κ anti-SSEA4-PE	BD Biosciences	560128
FITC Mouse IgM, κ Isotype Control RUO	BD Biosciences	553474
PE Mouse IgG3, κ Isotype Control RUO	BD Biosciences	559926
Chemicals, Peptides, and Recombinant Proteins		
IMDM	Sigma-Aldrich	I3390
Insulin	Sigma-Aldrich	I6634
Heparin	Choay	34869
Pool plasma AB	EFS	
Transferrin	Sigma-Aldrich	T4132
Glutamine	Life Technologies	25030081
SCF	MILTENYI	130-096-695
TPO	MILTENYI	130-094-013
Flt3l	MILTENYI	130-096-479
BMP4	MILTENYI	130-111-166
VEGF	MILTENYI	130-109-386
IL3	MILTENYI	130-095-068
IL6	MILTENYI	130-093-933
IL1 beta	MILTENYI	130-093-897
GCSF	MILTENYI	130-093-861
IGF1	MILTENYI	130-093-886
Matrigel hESC qualified	Corning	354277
DMEM/F-12	Gibco	C11330500BT
mTeSR™ Plus	*STEMCELL Technologies*	05825
ReLeSR™	*STEMCELL Technologies*	100-0484
D-PBS (Without Ca++ and Mg++)	Gibco	14190144
HSA	LFB	VIALEBEX
Methocult	Stemcell technologies	H4100

Collagenase B	ROCHE	11088815001
Growth factor-reduced Matrigel	Corning	354230
EBM-2 Medium	Lonza, Walkersville, USA	CC-3156
Critical Commercial Assays		
CellTrace™ CFSE	Thermofisher Scientific	C34570
Chromium Next GEM Single Cell 3' LT Kit v3.1	10X Genomics	1000325
Deposited Data		
Sequencing data supporting the findings of this study	Gene Expression Omnibus (GEO)	GSE224081
Crosse et al. sequencing data	GEO	GSE151877
BM human dataset	https://panglaodb.se/view_data.php?sra=SRA779509&srs=SRS3805267	SRR7881423
BM mouse dataset	https://panglaodb.se/view_data.php?sra=SRA653146&srs=SRS3044246	SRR6835854
Experimental Models: Cell Lines		
PCI-CAU hiPSC (aka internally PC045 RESCUE)	Phenocell	
PCI-1429 hiPSC	Phenocell	
FD136-25 hiPSC	Viville Lab	Lapillonne H et al. Haematologica. 2010 Oct;95(10):1651-9.
IMR90-16 hiPSC	Lapillonne et al., 2010	Lapillonne H et al. Haematologica. 2010 Oct;95(10):1651-9.
LAM01.005 hiPS	IPS CDTC core facility	
LAM02.002 hiPS	IPS CDTC core facility	
Mouse Stromal cells MS5	DSMZ	**ACC 441**
Experimental Models: Organisms/Strains		
mouse : NOD/SCID-LtSz-scid/scid (NOD/SCID)	Charles River Laboratories, L'Abresle, France	394
mouse : NOD.Cg-PrkdcscidIl2rgtm1Wjl/SzJ (NSG)	Charles River Laboratories, L'Abresle, France	614
Oligonucleotides		
TaqMan™ gene expression assays Human C-MYB	Thermofisher Scientific	4331182 Hs00193527_m1

TaqMan™ gene expression assays Human TCF7	Thermofisher Scientific	4331182 Hs01556515_m1
TaqMan™ gene expression assays Human RUNX1	Thermofisher Scientific	4331182 Hs00231079_m1
TaqMan™ gene expression assays Human HPRT1	Thermofisher Scientific	4331182 Hs01003267_m1
TaqMan™ gene expression assays Human CD19	Thermofisher Scientific	4331182 Hs00174333_m1
TaqMan™ gene expression assays Human HBG	Thermofisher Scientific	4331182 Hs00361131_g1
TaqMan™ gene expression assays Human HBB	Thermofisher Scientific	4331182 Hs00758889_s1
TaqMan™ gene expression assays Human HBE	Thermofisher Scientific	4331182 Hs00362216_m1
TaqMan™ gene expression assay Human GAPDH	Thermofisher Scientific	4331182 Hs02758991_g1
Taqman™ array Human hematopoiesis	Thermofisher Scientific	4418803
Software and Algorithms		
CellRanger 6.1.2.	10X Genomics	
SCTransform	github	https://github.com/satijalab/sctransform
SoupX	Young, M.D., Behjati, S. Gigascience (2020) doi: 10.1093/gigascience/giaa151 [61]	https://github.com/constantAmateur/SoupX
scHCL mapping	*Han, X. et al. Construction of a human cell landscape at singlecell level. Nature https://doi.org/10.1038/s41586-020-2157-4 (2020)*.[62]	https://github.com/ggjlab/scHCL
sc MCA mapping	Han et al., 2018, Cell. DOI:https://doi.org/10.1016/j.cell.2018.02.001 [63]	https://github.com/ggjlab/scMCA
Seurat	[64]	https://github.com/satijalab/seurat
JMP	SAS, Institute Inc., Cary, USA	8.0
PRISM	GRAPHPAD	8.0
Flowjo	BD	X

Figure 1

LITTERATURE MINING

INPUT VARIABLES

Concentrations of growth factors involved in mesoderm commitment : **BMP4, VEGF**

Concentrations of cytokines involved in hematopoietic commitment

SCF, TPO, FLT3, IL3, IL6, IL1, GCSF, IGF

OUTPUT VARIABLES

Cell amplification

Cell characterization by flow cytometry

CD34, CD117, CD43, CD45, CD13, CD33, CD38, CD90, CD109, HLA-DR

Long Term Culture-Initiating Cell (LTC-IC) frequency

STATISTICAL STEPS

CUSTOM DESIGN

16 experiments displaying statistically different concentrations of cytokines and growth factors

Cell amplification : 16 results

Flow cytometry : 144 results

LTC-IC frequency : 16 results

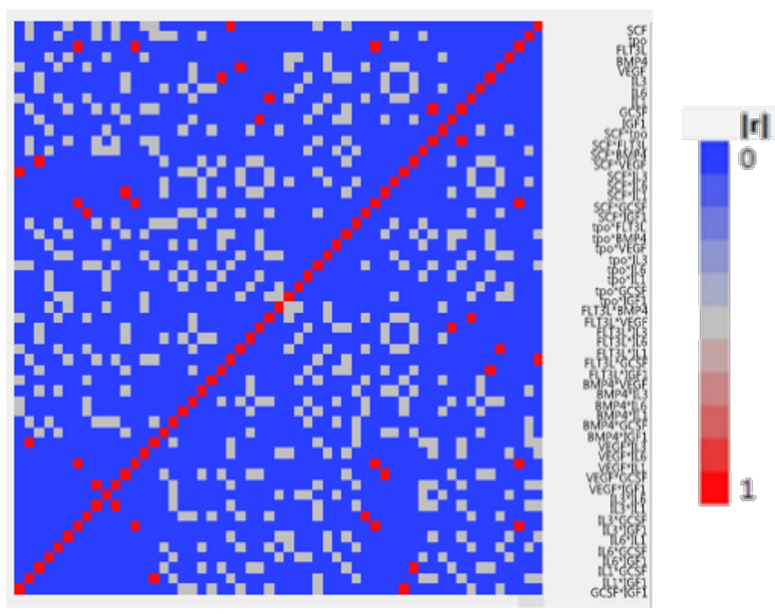

Mathematical modeling of the input/output variable interactions

Three combinations of cytokines were selected to obtain highly amplifying cells harboring **CD34, CD117, CD43, CD45** hematopoietic commitment

RESULTS

Flow cytometric analysis of D17 EBs

Tested on two different hiPSC lines, FD136-25 and IMR90

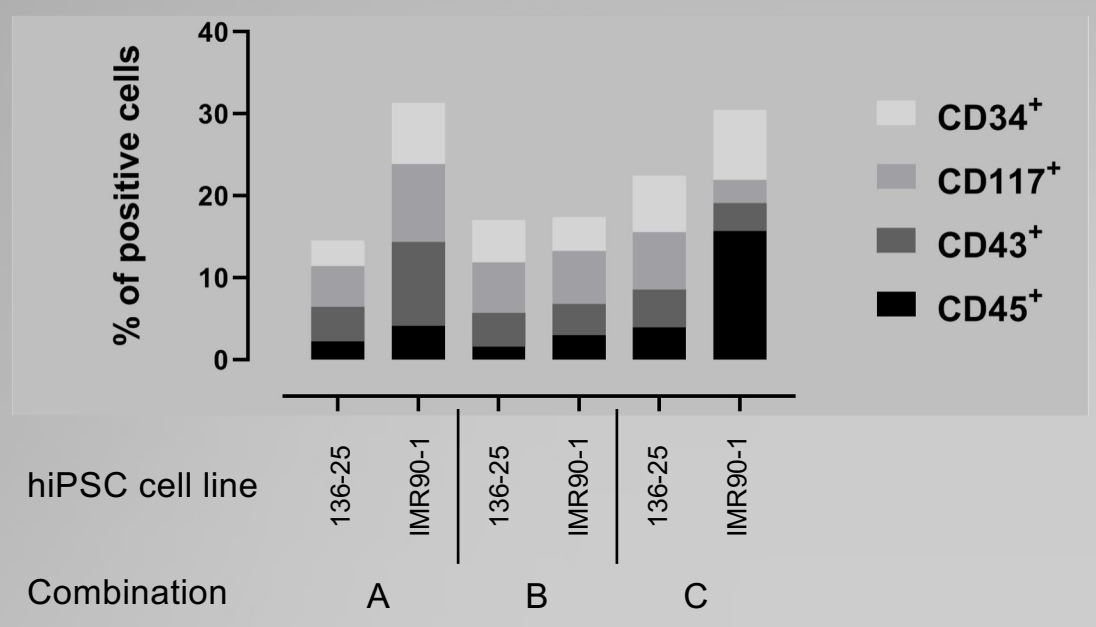

NOD SCID primary recipients

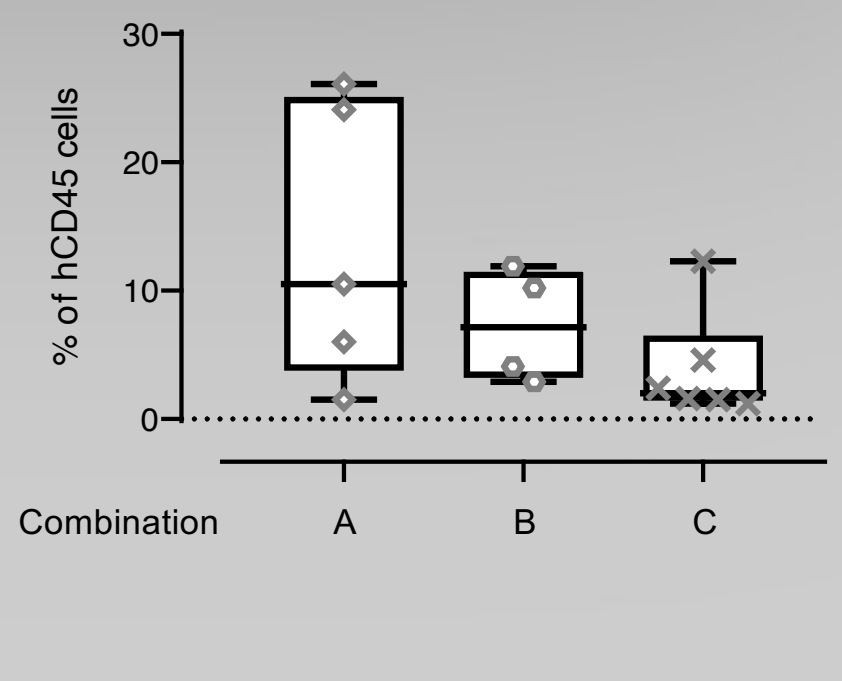

Figure 2

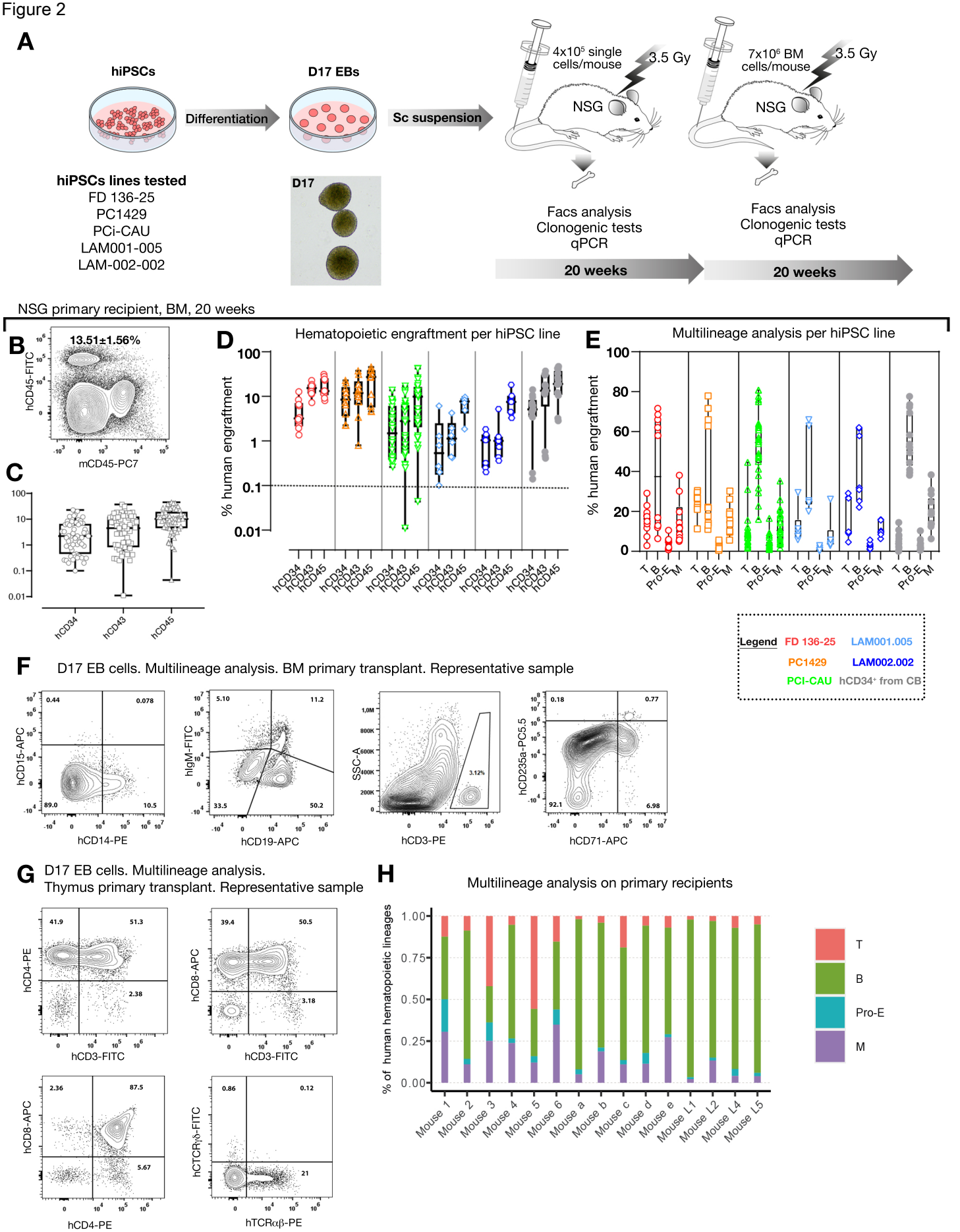
A
hiPSCs
Differentiation
D17 EBs
Sc suspension
hiPSCs lines tested
FD 136-25
PC1429
PCi-CAU
LAM001-005
LAM-002-002
D17
4x10⁵ single cells/mouse
3.5 Gy
NSG
7x10⁶ BM cells/mouse
3.5 Gy
NSG
Facs analysis
Clonogenic tests
qPCR
20 weeks
Facs analysis
Clonogenic tests
qPCR
20 weeks
NSG primary recipient, BM, 20 weeks
B
13.51±1.56%
hCD45-FITC
mCD45-PC7
C
hCD34
hCD43
hCD45
D
Hematopoietic engraftment per hiPSC line
% human engraftment
E
Multilineage analysis per hiPSC line
% human engraftment
T B Pro-E M
Legend
FD 136-25
LAM001.005
PC1429
LAM002.002
PCI-CAU
hCD34+ from CB
F
D17 EB cells. Multilineage analysis. BM primary transplant. Representative sample
hCD15-APC
hCD14-PE
hIgM-FITC
hCD19-APC
SSC-A
hCD3-PE
hCD235a-PC5.5
hCD71-APC
G
D17 EB cells. Multilineage analysis.
Thymus primary transplant. Representative sample
hCD4-PE
hCD3-FITC
hCD8-APC
hCD3-FITC
hCD8-APC
hCD4-PE
hTCRγδ-FITC
hTCRαβ-PE
H
Multilineage analysis on primary recipients
% of human hematopoietic lineages
Mouse 1
Mouse 2
Mouse 3
Mouse 4
Mouse 5
Mouse 6
Mouse a
Mouse b
Mouse c
Mouse d
Mouse e
Mouse L1
Mouse L2
Mouse L4
Mouse L5
T
B
Pro-E
M

Figure 3

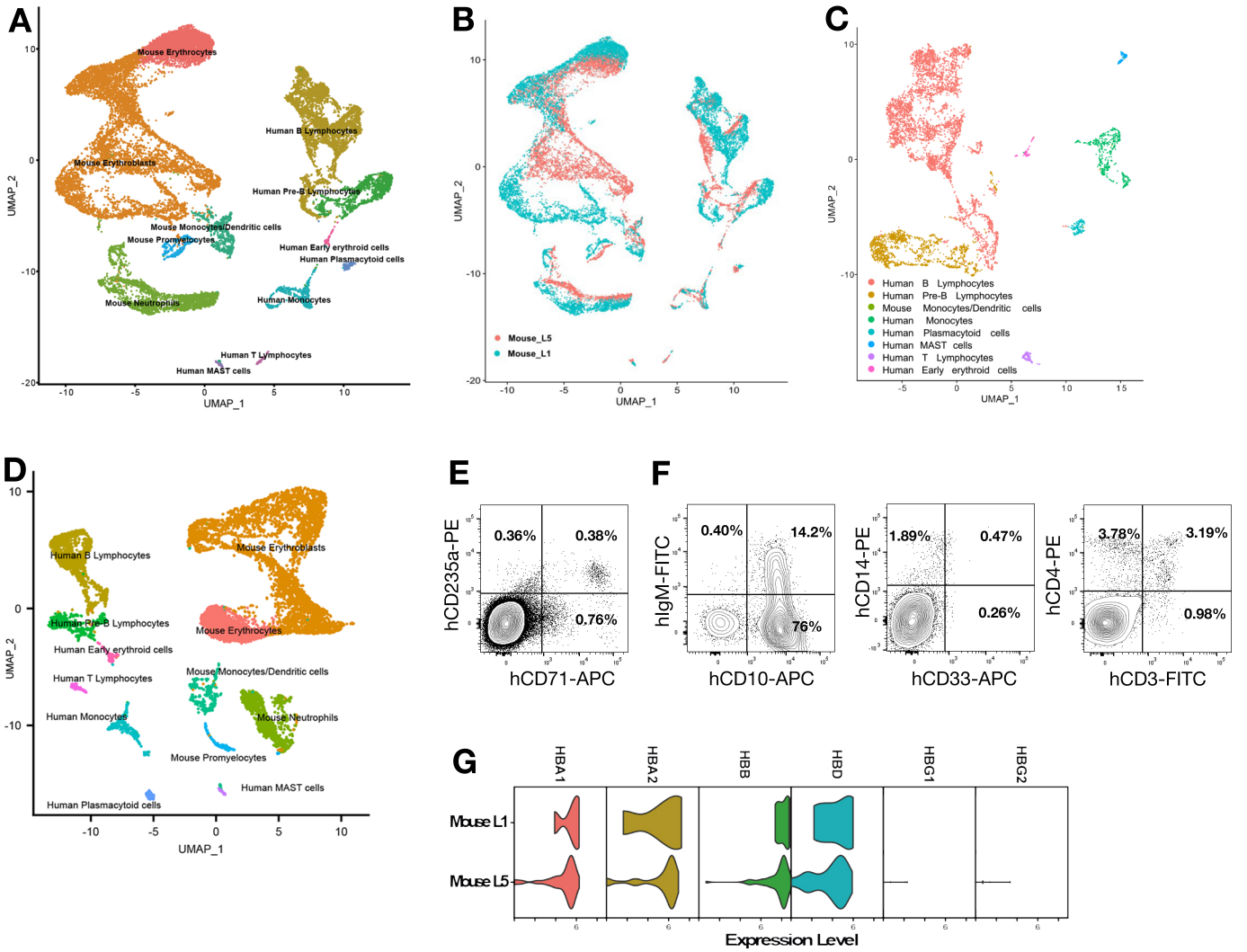
A
Mouse Erythrocytes
Mouse Erythroblasts
Human B Lymphocytes
Human Pre-B Lymphocytes
Mouse Monocytes/Dendritic cells
Mouse Promyelocytes
Human Early erythroid cells
Human Plasmacytoid cells
Mouse Neutrophils
Human Monocytes
Human T Lymphocytes
Human MAST cells
UMAP_1
UMAP_2
B
Mouse_L5
Mouse_L1
C
Human B Lymphocytes
Human Pre-B Lymphocytes
Mouse Monocytes/Dendritic cells
Human Monocytes
Human Plasmacytoid cells
Human MAST cells
Human T Lymphocytes
Human Early erythroid cells
D
Human B Lymphocytes
Mouse Erythroblasts
Human Pre-B Lymphocytes
Mouse Erythrocytes
Human Early erythroid cells
Mouse Monocytes/Dendritic cells
Human T Lymphocytes
Human Monocytes
Mouse Neutrophils
Mouse Promyelocytes
Human MAST cells
Human Plasmacytoid cells
E
hCD235a-PE
hCD71-APC
0.36%
0.38%
0.76%
F
hIgM-FITC
hCD10-APC
0.40%
14.2%
76%
hCD14-PE
hCD33-APC
1.89%
0.47%
0.26%
hCD4-PE
hCD3-FITC
3.78%
3.19%
0.98%
G
HBA1
HBA2
HBB
HBD
HBG1
HBG2
Mouse L1
Mouse L5
Expression Level

Figure 4

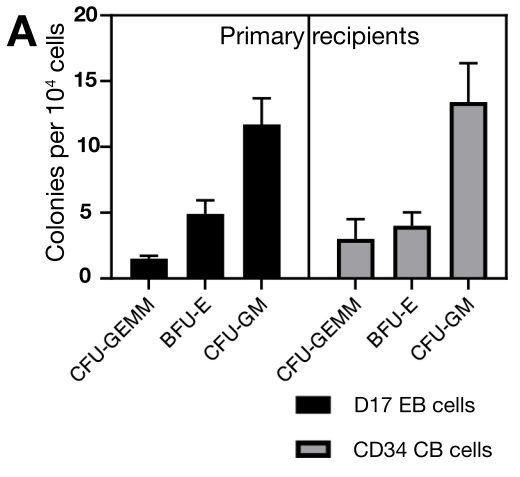

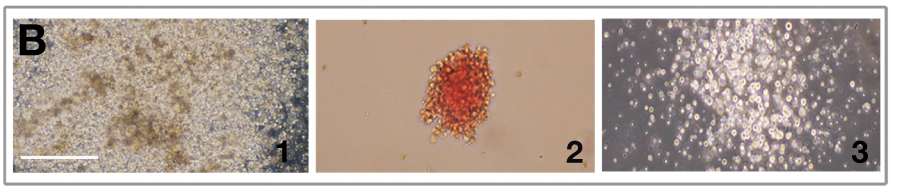

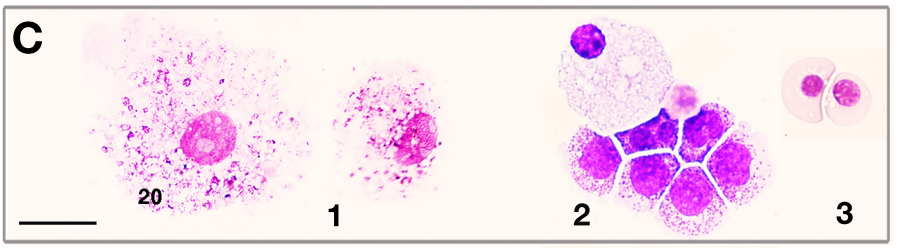

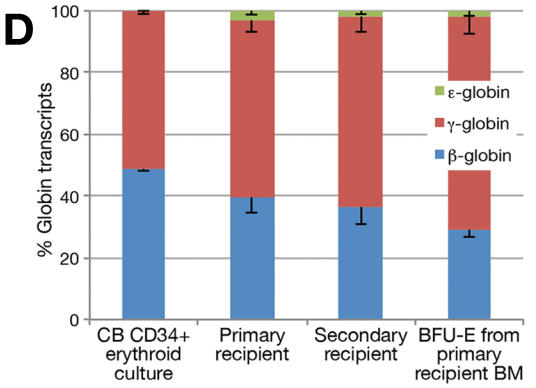

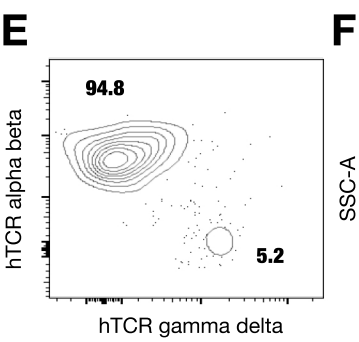

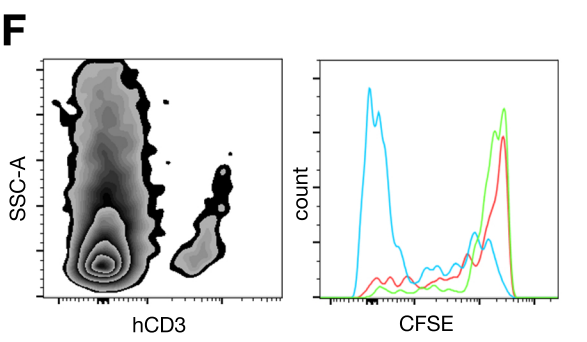

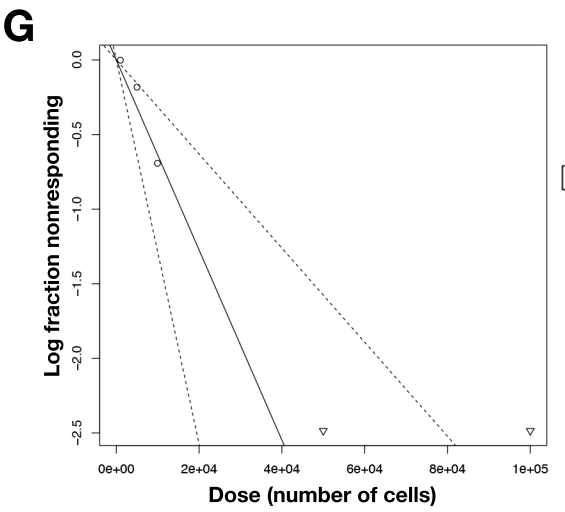

	Lower	Estimate	Upper
D17	31715	15700	7773

Figure 5

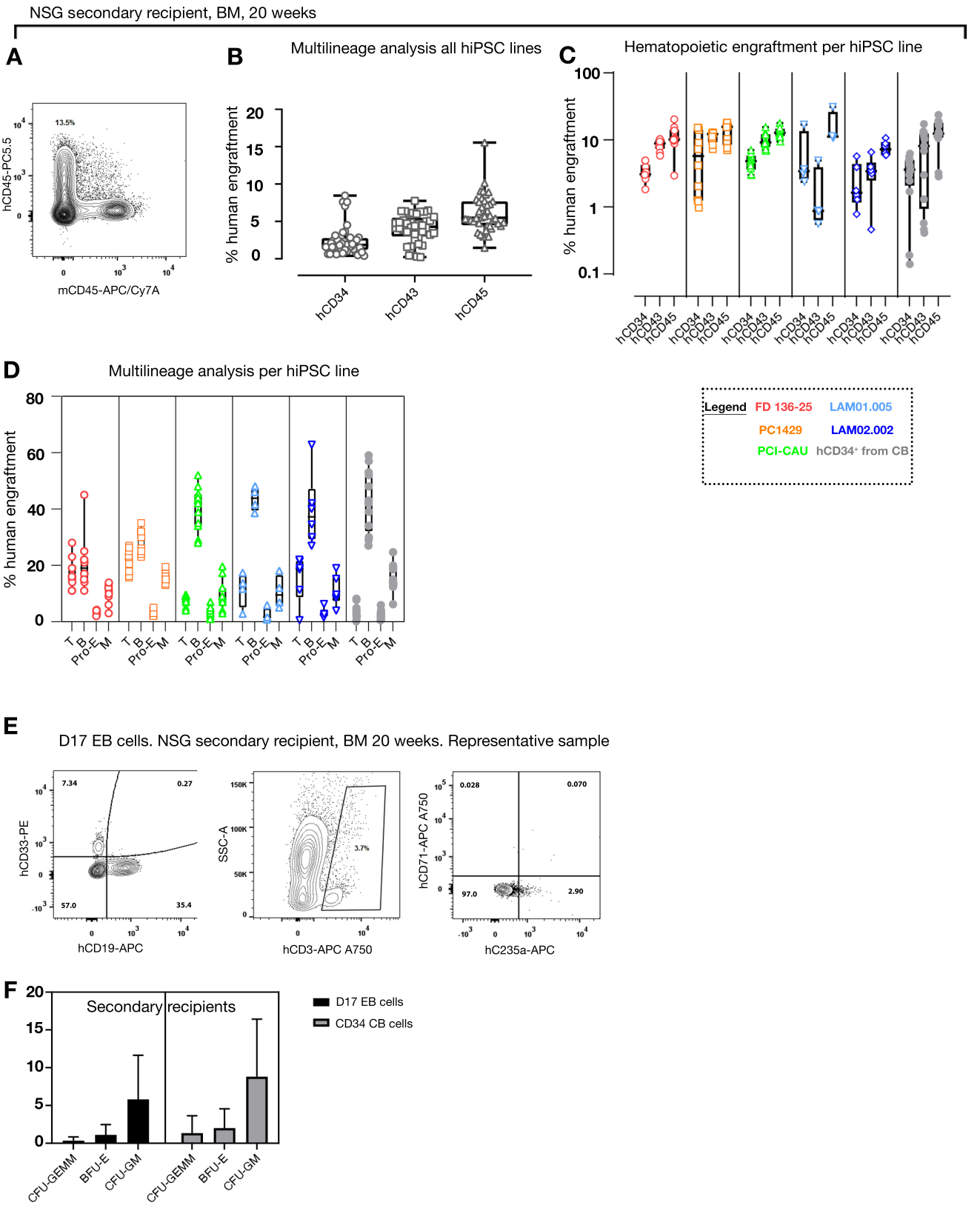
NSG secondary recipient, BM, 20 weeks
A
13.5%
hCD45-PC5.5
mCD45-APC/Cy7A
B
Multilineage analysis all hiPSC lines
% human engraftment
hCD34
hCD43
hCD45
C
Hematopoietic engraftment per hiPSC line
% human engraftment
hCD34
hCD43
hCD45
D
Multilineage analysis per hiPSC line
% human engraftment
T
B
Pro-E
M
Legend
FD 136-25
LAM01.005
PC1429
LAM02.002
PCI-CAU
hCD34+ from CB
E
D17 EB cells. NSG secondary recipient, BM 20 weeks. Representative sample
7.34
0.27
57.0
35.4
hCD33-PE
hCD19-APC
SSC-A
3.7%
hCD3-APC A750
0.028
0.070
97.0
2.90
hCD71-APC A750
hC235a-APC
F
Secondary recipients
D17 EB cells
CD34 CB cells
CFU-GEMM
BFU-E
CFU-GM

Figure 6

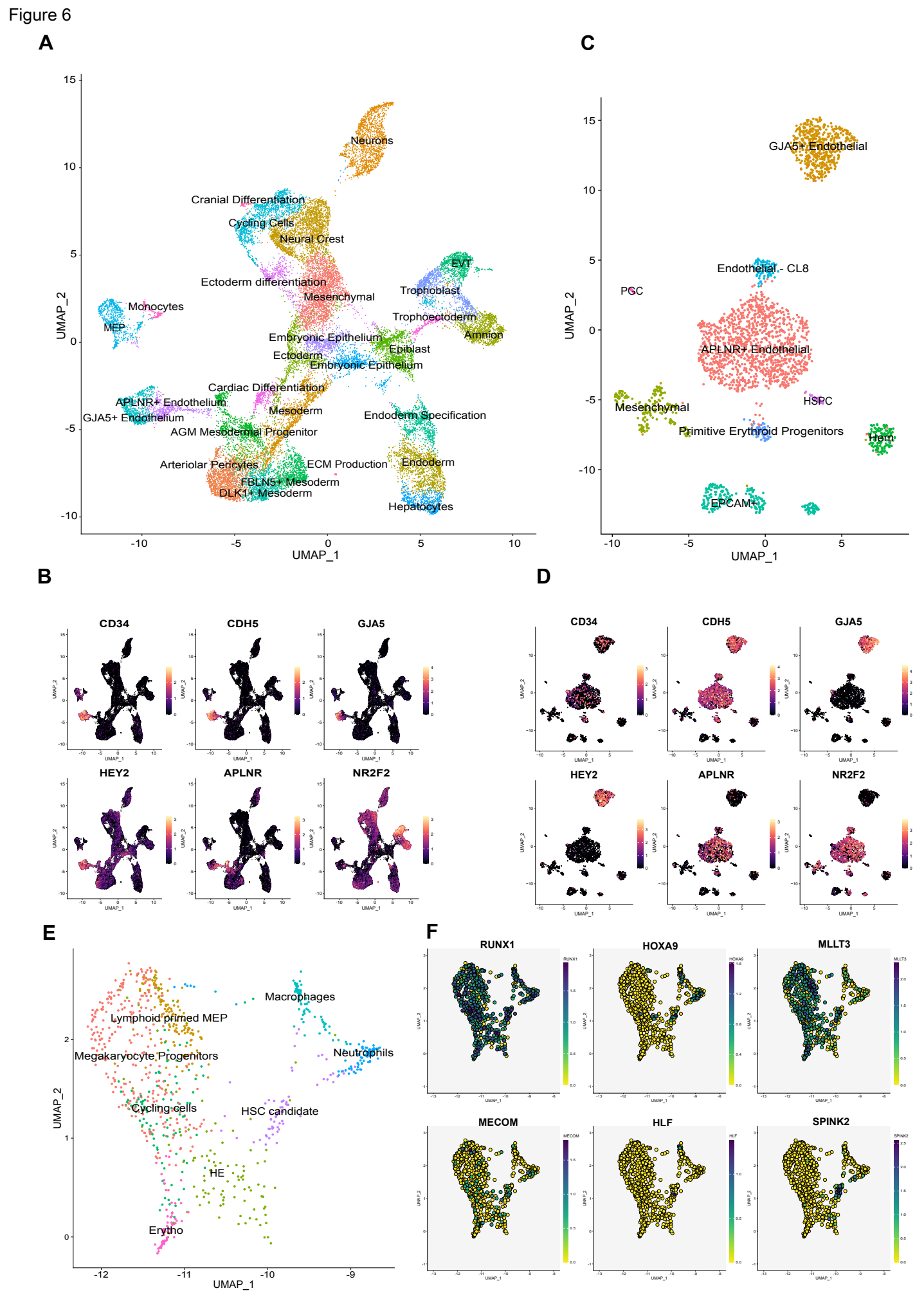
A
Neurons
Cranial Differentiation
Cycling Cells
Neural Crest
Ectoderm differentiation
Mesenchymal
EVT
Trophoblast
Trophoectoderm
Amnion
Monocytes
MEP
Embryonic Epithelium
Epiblast
Ectoderm
Embryonic Epithelium
Cardiac Differentiation
APLNR+ Endothelium
GJA5+ Endothelium
Mesoderm
Endoderm Specification
AGM Mesodermal Progenitor
Arteriolar Pericytes
ECM Production
Endoderm
FBLN5+ Mesoderm
DLK1+ Mesoderm
Hepatocytes
UMAP_1
UMAP_2
C
GJA5+ Endothelial
Endothelial - CL8
PGC
APLNR+ Endothelial
Mesenchymal
HSPC
Primitive Erythroid Progenitors
Heme
EPCAM+
UMAP_1
UMAP_2
B
CD34
CDH5
GJA5
HEY2
APLNR
NR2F2
D
CD34
CDH5
GJA5
HEY2
APLNR
NR2F2
E
Macrophages
Lymphoid primed MEP
Megakaryocyte Progenitors
Neutrophils
Cycling cells
HSC candidate
HE
Erytho
UMAP_1
UMAP_2
F
RUNX1
HOXA9
MLLT3
MECOM
HLF
SPINK2

Figure 7

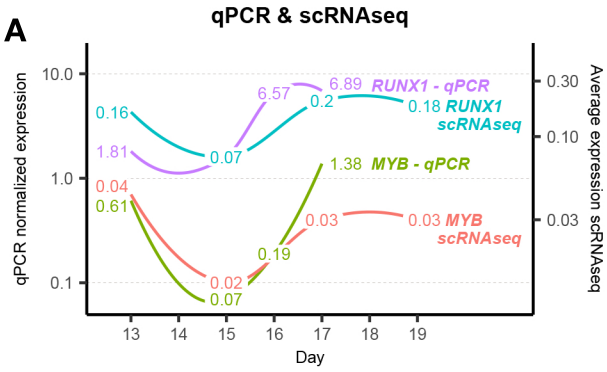
A
qPCR & scRNAseq
qPCR normalized expression
Average expression scRNAseq
Day
RUNX1 - qPCR
RUNX1 scRNAseq
MYB - qPCR
MYB scRNAseq

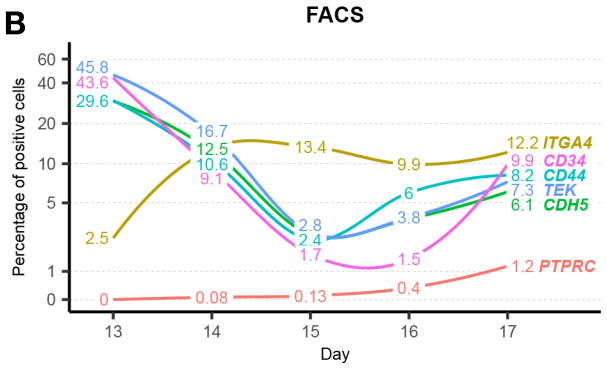
B
FACS
Percentage of positive cells
Day
ITGA4
CD34
CD44
TEK
CDH5
PTPRC

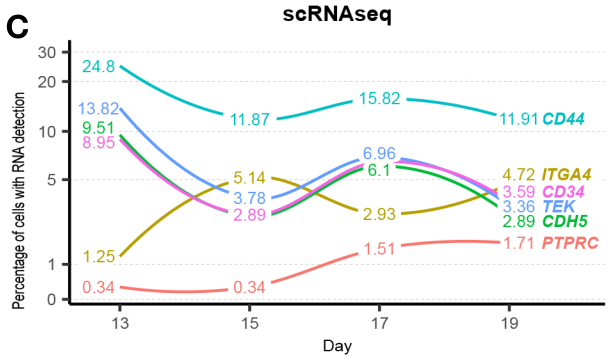
C
scRNAseq
Percentage of cells with RNA detection
Day
CD44
ITGA4
CD34
TEK
CDH5
PTPRC

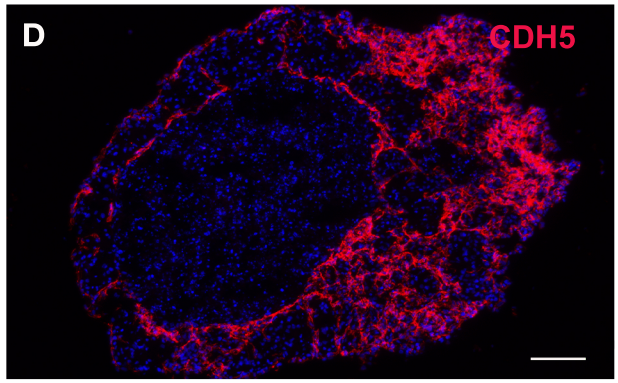
D
CDH5

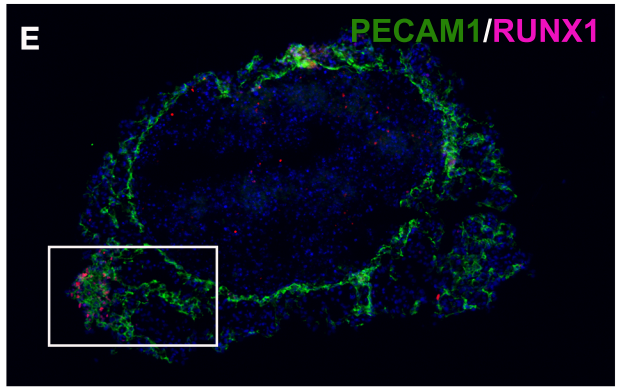
E
PECAM1/RUNX1

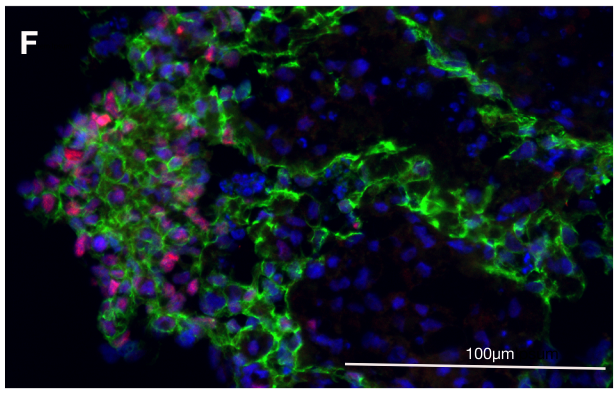
F
100µm

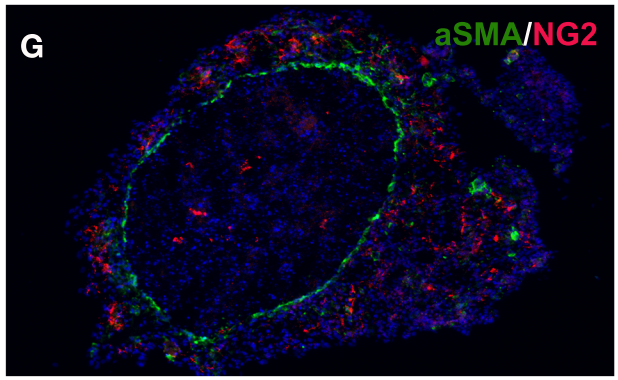
G
aSMA/NG2

SUPPLEMENTAL FIGURES AND TABLES (PIAU ET AL.,)

SUPPLEMENTAL FIGURES

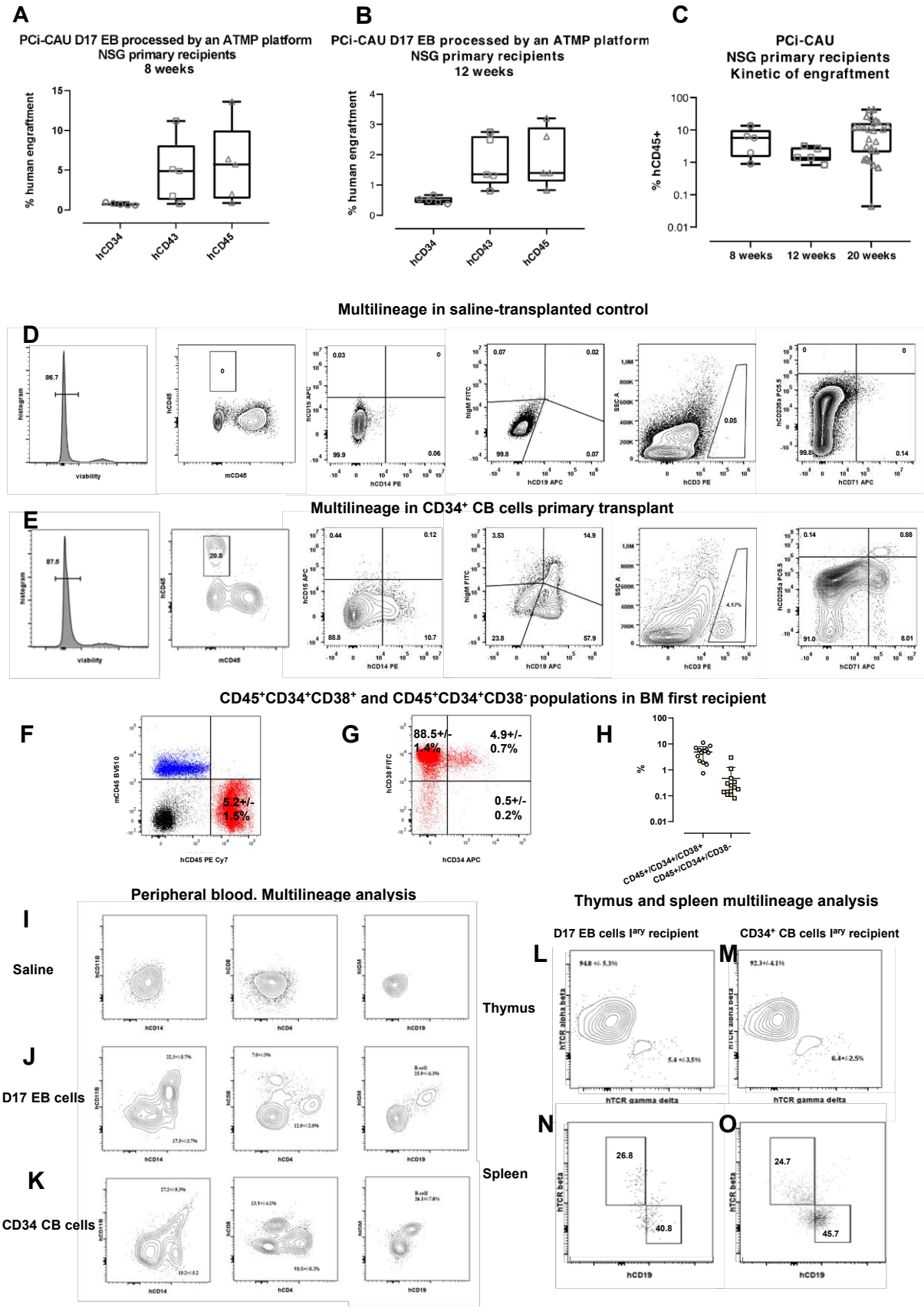
A
PCi-CAU D17 EB processed by an ATMP platform
NSG primary recipients
8 weeks
% human engraftment
hCD34
hCD43
hCD45
B
PCi-CAU D17 EB processed by an ATMP platform
NSG primary recipients
12 weeks
% human engraftment
hCD34
hCD43
hCD45
C
PCi-CAU
NSG primary recipients
Kinetic of engraftment
% hCD45+
8 weeks
12 weeks
20 weeks
Multilineage in saline-transplanted control
D
Multilineage in CD34+ CB cells primary transplant
E
CD45+CD34+CD38+ and CD45+CD34+CD38- populations in BM first recipient
F
hCD45 PE Cy7
5.2+/- 1.5%
G
hCD34 APC
88.5+/- 1.4%
4.9+/- 0.7%
0.5+/- 0.2%
H
%
CD45+/CD34+/CD38+
CD45+/CD34+/CD38-
Peripheral blood. Multilineage analysis
I
Saline
J
D17 EB cells
K
CD34 CB cells
Thymus and spleen multilineage analysis
D17 EB cells Iary recipient
CD34+ CB cells Iary recipient
L
M
Thymus
N
O
Spleen
hTCR gamma delta
hTCR alpha beta
hTCR beta
hCD19
26.8
40.8
24.7
45.7

Supplementary Figure 1 is related to Figure 2.
***In vivo* engraftment of D17 human EB cells in primary NSG mice.**

(A-B) D17 EB cells from PCi-CAU, prepared by the Atlantic Bio GMP platform (Nantes, France), (A) multilineage analysis at 8 weeks (5 mice, n=1). (B) at 12 weeks (n=5, 1 experiment). Post grafts. FACS results are expressed as % of $hCD34^+$, $hCD43^+$, and $hCD45^+$. Wilcoxon Mann-Whitney test. Data are mean±SD or SEM depending on the number of independent experiments

(C) Kinetics of cell grafting at 8, 12, and 20 weeks (n=5 mice, 5 mice, 1 experiment for 8 and 12 weeks respectively and, n=59 mice, 14 independent experiments) post-transplantation resulting from pooling of in-house and Atlantic Bio GMP platform results. FACS results are expressed as % of $hCD45^+$.
(D) human Multilineage engraftment. Flow cytometric analysis of BM. Representative control (saline-injected) primary recipients at 20 weeks (n=16, 8 independent experiments) showing Myeloid (M), B, T and Pro-erythroid cells (Pro-E). $hCD45^+$ population was analyzed for expression of hCD14/hCD15 (monocytes/macrophages), hCD19/hIgM (B cells), and hCD3 (T cells). hCD71/hCD235a (ProE) analysis was performed on whole BM cells.

(E) Representative primary recipients transplanted with 4.10^5 $CD34^+$ CB cells (n=13 mice, 3 independent experiments). Same analysis as in (D).

(F) Representative FACS analysis of D17 grafts BM for human and mouse CD45 expression.

(G) Representative FACS analysis of D17 grafts BM for human CD34 and CD38 expression. Numbers indicate mean ± SEM of 14 mice analyzed. (n=14, 2 independent experiments).

(H) Representation of hCD45+ hCD34+ hCD38+ and hCD45+ hCD34+ hCD38- populations. (n=14, 2 independent experiments).

(I-K) Analysis of NSG peripheral blood in control (I, n=16, 8 independent experiments), D17EB (J, n=59, 14 independent experiments) and $CD34^+$ CB cell (K, n=13, 3 independent experiments)-transplanted mice. Primary recipients at 20 weeks. Myeloid (hCD11B/CD14) and lymphoid (CD19/IgM and CD4/CD8) lineages in peripheral blood. Analyzes were performed on human $CD45^+$ cells, except for saline-transplanted recipients.

(L-O) Analysis of NSG thymus (J, K) and spleen (L, M). Primary recipients at 20 weeks.

(L-M) Representative thymuses from NSG mice transplanted with D17 EB cells (H, 59 mice, n=14) or $CD34^+$ CB cells (13 mice, n=3). hTCR alpha/beta and gamma/delta flow cytometric analysis. The CD3-gated thymus cells had a large amount of TCR alpha-beta cells, which was very similar to the amount on the $CD34^+$ CB cells.

(N-O) Representative NSG spleen. hTCR beta and hCD19 flow cytometric analysis. (K) D17 EB cell-transplanted NSG (n=59, 14 independent experiments). (L) $CD34^+$ CB cells-transplanted NSG (13 mice, n=3). The $hCD45^+$-gated splenocytes exhibited a B- or T-lymphoid phenotype, with similar ratios as the $CD34^+$ CB cells.

Data are presented as box plots and are mean ± SD or SEM according to the number of independent experiments. Wilcoxon Mann-Whitney test.

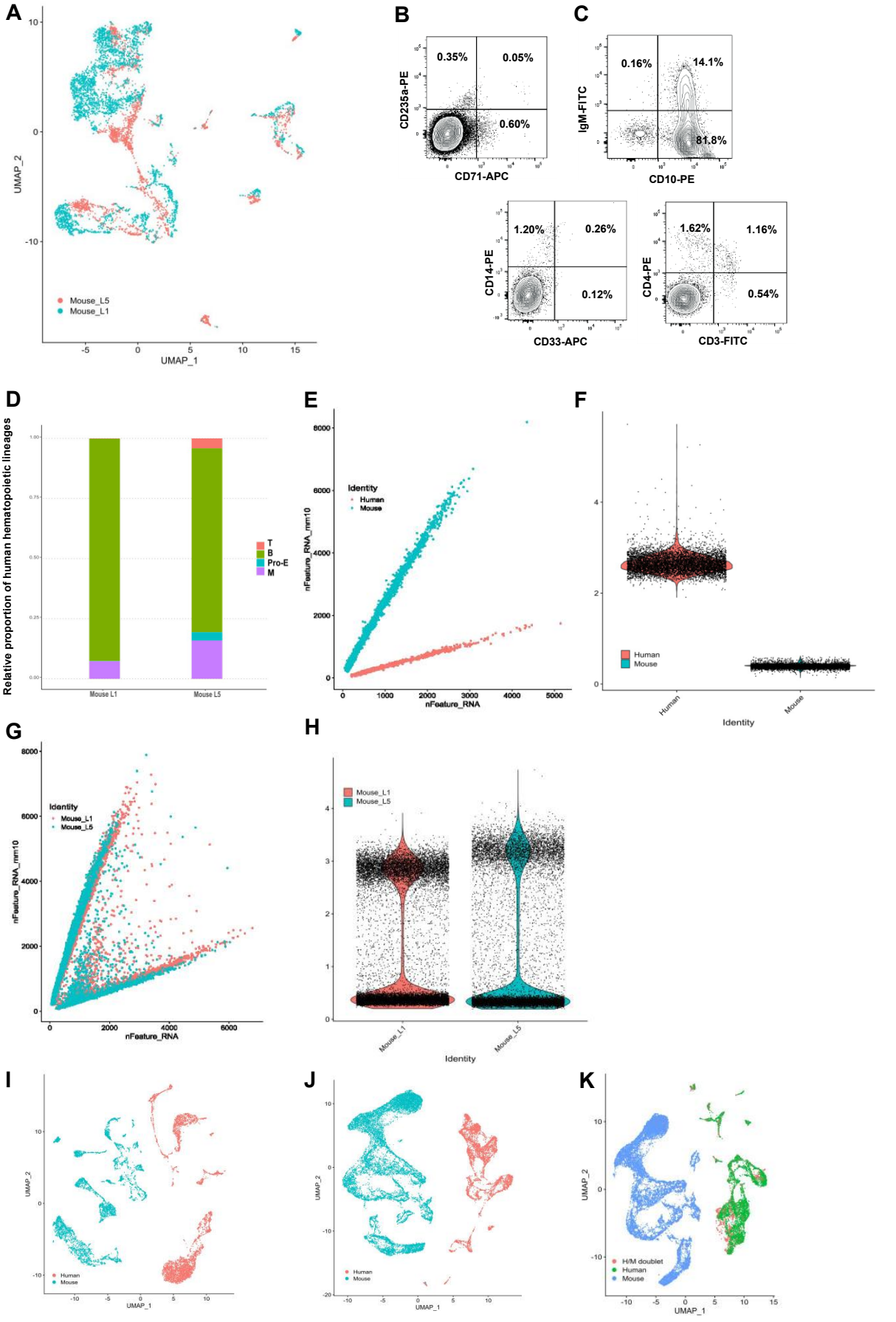
A
UMAP_2
UMAP_1
Mouse_L5
Mouse_L1
B
CD235a-PE
CD71-APC
0.35%
0.05%
0.60%
C
IgM-FITC
CD10-PE
0.16%
14.1%
81.8%
CD14-PE
CD33-APC
1.20%
0.26%
0.12%
CD4-PE
CD3-FITC
1.62%
1.16%
0.54%
D
Relative proportion of human hematopoietic lineages
T
B
Pro-E
M
Mouse L1
Mouse L5
E
Identity
Human
Mouse
nFeature_RNA_mm10
nFeature_RNA
F
Human
Mouse
Identity
G
Identity
Mouse_L1
Mouse_L5
nFeature_RNA_mm10
nFeature_RNA
H
Mouse_L1
Mouse_L5
Identity
I
UMAP_2
UMAP_1
Human
Mouse
J
UMAP_2
UMAP_1
Human
Mouse
K
UMAP_2
UMAP_1
H/M doublet
Human
Mouse

Supplementary Figure 2 is related to Figure 3.

ScRNA-seq analysis of the BM from two representative mice engrafted with D17 EB cells 20 weeks after transplant and separation strategy for human and mouse cells in scRNA-Seq.

(A) UMAP embedding of a merged dataset of human cells in the two engrafted BM datasets (primary mice L1 and L5) colored by sample.

(B, C) Bone marrow chimerism of primary mouse L1 transplanted with D17 EB cells at 20 weeks. (B) Erythroid cells (hCD235a/hCD71) from total BM cells. (C) B cells ($hIgM^+/hCD10^+$), neutrophils ($hCD33^+/hCD14^+$), and T cells ($hCD4^+/hCD3^+$) from CD45+ cells.

(D) Stacked histogram of the relative proportions of the major hematopoietic cell populations detected by scRNAseq in the transplanted BM of L1 and L5 mice. Myeloid (M), Pro-erythroid cells (Pro-E), B cells, and T cells.

(E, G) Scatter plot of the number of genes detected in each cell on the grch38 and the mm10 assembly in the control dataset (E) and the engrafted mouse dataset (G)

(F, H) Violin Plot of the ratio of genes detected with the grch38 assembly and the mm10 assembly in the control dataset (F) and the engrafted mouse dataset (H)

(I, J) UMAP embedding of the cells profiled by scRNA-Seq in the control dataset (I) and the engrafted mouse dataset (J)

(K) UMAP embeddings of the cells in the engrafted mouse dataset before filtering out doublets.

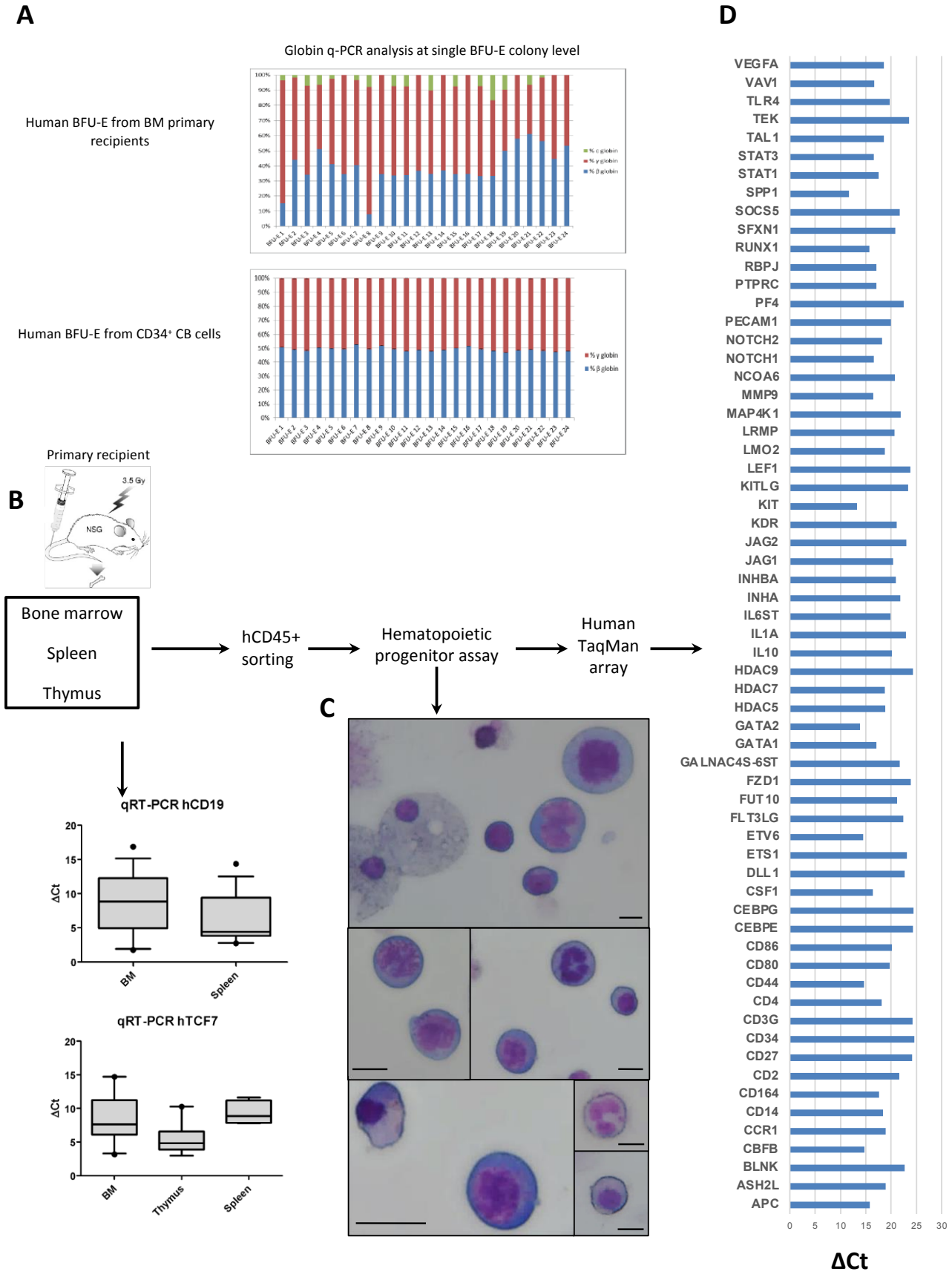
A
Globin q-PCR analysis at single BFU-E colony level
Human BFU-E from BM primary recipients
% ε globin
% γ globin
% β globin
Human BFU-E from CD34+ CB cells
% γ globin
% β globin
B
Primary recipient
3.5 Gy
NSG
Bone marrow
Spleen
Thymus
hCD45+ sorting
Hematopoietic progenitor assay
Human TaqMan array
qRT-PCR hCD19
ΔCt
BM
Spleen
qRT-PCR hTCF7
ΔCt
BM
Thymus
Spleen
C
D
VEGFA
VAV1
TLR4
TEK
TAL1
STAT3
STAT1
SPP1
SOCS5
SFXN1
RUNX1
RBPJ
PTPRC
PF4
PECAM1
NOTCH2
NOTCH1
NCOA6
MMP9
MAP4K1
LRMP
LMO2
LEF1
KITLG
KIT
KDR
JAG2
JAG1
INHBA
INHA
IL6ST
IL1A
IL10
HDAC9
HDAC7
HDAC5
GATA2
GATA1
GALNAC4S-6ST
FZD1
FUT10
FLT3LG
ETV6
ETS1
DLL1
CSF1
CEBPG
CEBPE
CD86
CD80
CD44
CD4
CD3G
CD34
CD27
CD2
CD164
CD14
CCR1
CBFB
BLNK
ASH2L
APC
0 5 10 15 20 25 30
ΔCt

Supplementary Figure 3 is related to Figure 4.

Molecular characterization of the grafted cells, globin RT-qPCR analysis from BFU-E at the single colony level.

(A) Up: Individual BFU-E colonies from BM cell cultures of primary recipients (approximately 18% of total colonies). Down: $CD34^+$ human CB cells. Shown is the ratio of beta (blue), gamma (red) and epsilon (green) globin. CD34 CB cells give rise to colonies with a homogeneous ratio of beta- and gamma-globin, whereas BM cells give rise to a more diverse globin composition with a weak expression of epsilon-globin.

(B) qRT-PCR analysis for hCD19 (B lymphocyte surface antigen B4, B cell-specific marker) and hTCF7, a T-cell-specific marker, was performed on thymus, spleen, and bone marrow.
For each gene, delta Ct is the mean ± SEM of 3 independent experiments.

(C) Cytospins. May Grünwald-Giemsa staining of cells isolated from clonogenic assays in primary and secondary recipients. Scale bars represent 10µm.

(D) Representative qRT-PCR results obtained with a TaqMan® Array Human Hematopoiesis 96-well plate from $hCD45^+$ BM cells.

Figure S4

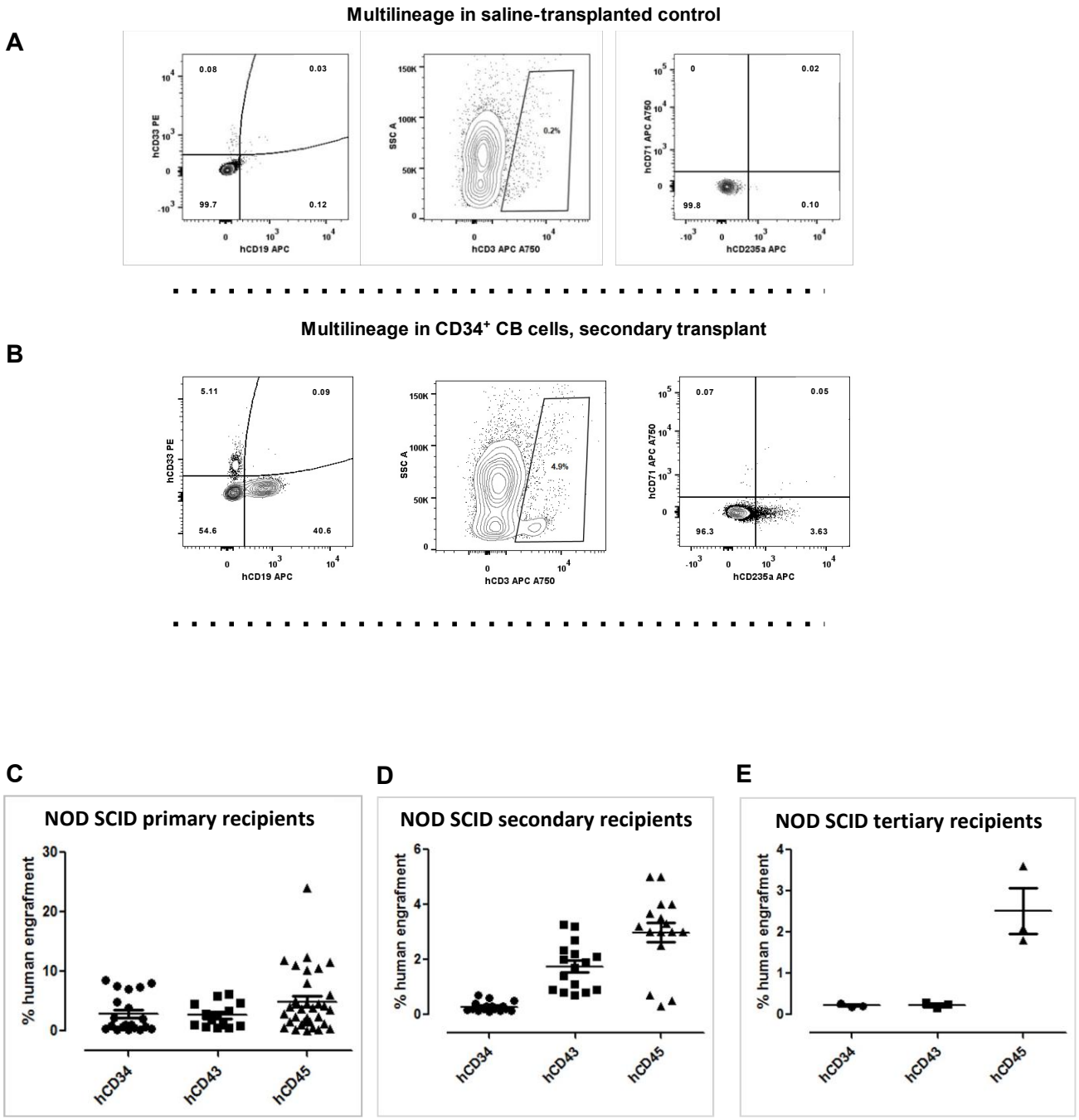
A
Multilineage in saline-transplanted control
hCD33 PE
hCD19 APC
0.08
0.03
99.7
0.12
SSC A
hCD3 APC A750
0.2%
hCD71 APC A750
hCD235a APC
0
0.02
99.8
0.10
B
Multilineage in CD34+ CB cells, secondary transplant
5.11
0.09
54.6
40.6
4.9%
0.07
0.05
96.3
3.63
C
NOD SCID primary recipients
% human engrafment
hCD34
hCD43
hCD45
D
NOD SCID secondary recipients
E
NOD SCID tertiary recipients

Supplementary Figure 4 is related to Figure 5.

Secondary transplants in NSG mice; representative recipients for saline and CD34$^+$ CB cells and hematopoietic engraftment in primary, secondary and tertiary NOD-SCID recipients at 20 weeks post-graft.

(A) Flow cytometric analysis of a representative control (saline-injected) secondary recipient. Myeloid (hCD33), B lymphoid (hCD19), T lymphoid (hCD3) and pro-erythroid (hCD71/hCD235a) lineages. Myeloid and lymphoid cells are analyzed from hCD45$^+$ gated BM cells whereas Pro-E hCD71/hCD235a was analyzed on whole BM cells. (n=16, 8 independent experiments)

(B) Representative primary recipients transplanted with 7.10^6 CD34$^+$ CB cells (n= 13, 3 independent experiments). Same analysis as in (D).

(C) Primary NOD-SCID recipient inoculated with 4.10^5 D17 EB cells (n=20, 3 independent experiments).

(D) Secondary NOD-SCID recipients inoculated with 7.10^6 BM cells from primary recipients (n= 16, 2 independent experiments).

(E) Tertiary NOD-SCID recipient inoculated with 7.10^6 BM cells from secondary recipients (n=3, 1 experiment).

Data are presented as box plots and are mean ± SD or SEM according to the number of independent experiments. Wilcoxon Mann-Whitney test.

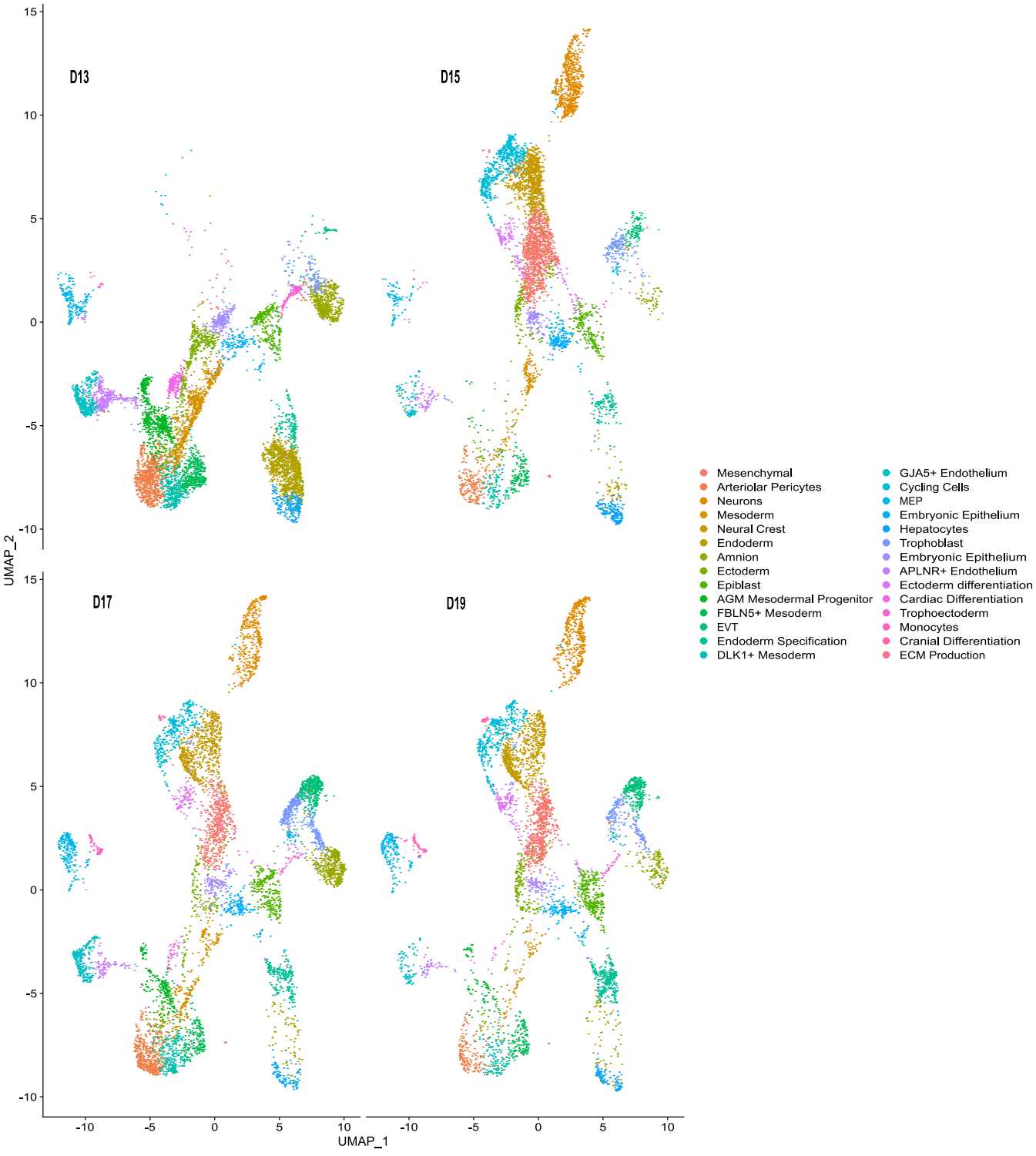
D13
D15
D17
D19
UMAP_2
UMAP_1
15
10
5
0
-5
-10
Mesenchymal
Arteriolar Pericytes
Neurons
Mesoderm
Neural Crest
Endoderm
Amnion
Ectoderm
Epiblast
AGM Mesodermal Progenitor
FBLN5+ Mesoderm
EVT
Endoderm Specification
DLK1+ Mesoderm
GJA5+ Endothelium
Cycling Cells
MEP
Embryonic Epithelium
Hepatocytes
Trophoblast
Embryonic Epithelium
APLNR+ Endothelium
Ectoderm differentiation
Cardiac Differentiation
Trophoectoderm
Monocytes
Cranial Differentiation
ECM Production

Supplementary Figure 5 is related to Figure 6.

Identification and evolution of the cell populations detected in the embryoid bodies by scRNA-Seq at D13, 15, 17 and 19.

Repartition of the cells from each timepoint on the UMAP embedding of the EBs. EVT: Extravillous Trophoblast. MEP: Megakaryocyte-Erythroid Progenitors. ECM: Extracellular Matrix. AGM: Aorta-Gonad-Mesonephros.

A

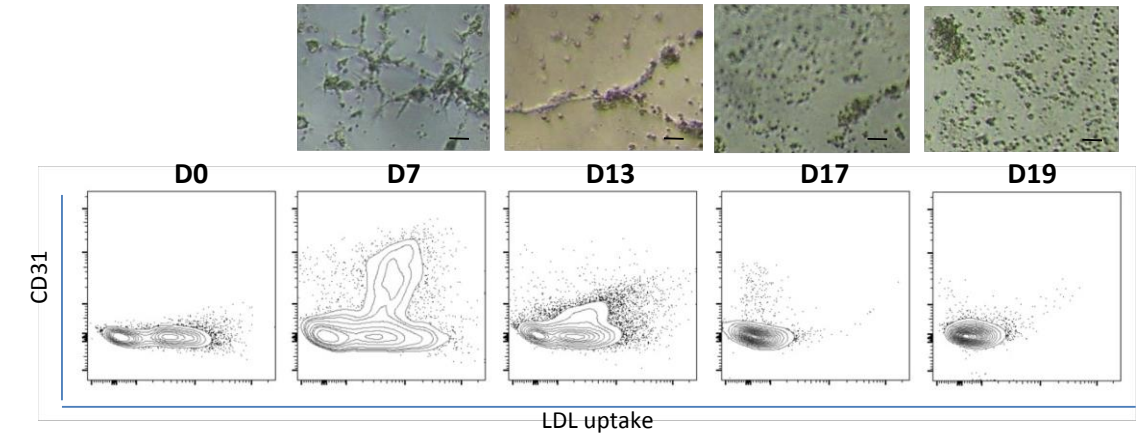

B

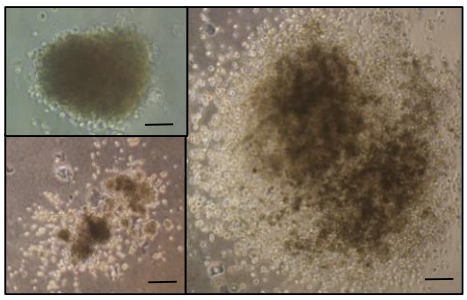

C

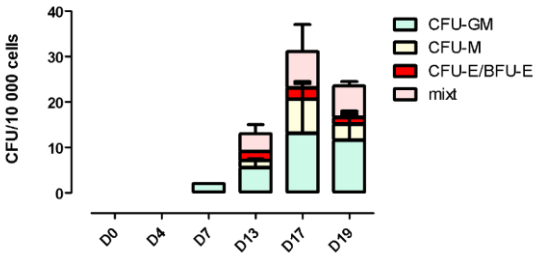

	D0	D7	D13	D17	D19
CFU/10 000 seeded cells	0	0.6 +/- 0.7	13 +/- 2.1	30.2 +/- 5.7	24.3 +/- 3.6
CFU/10 000 seeded CD34+ cells	0	1.8 +/- 2.1	82.7 +/-13.4	203.8 +/- 38.4	198.2+/-29.4

D

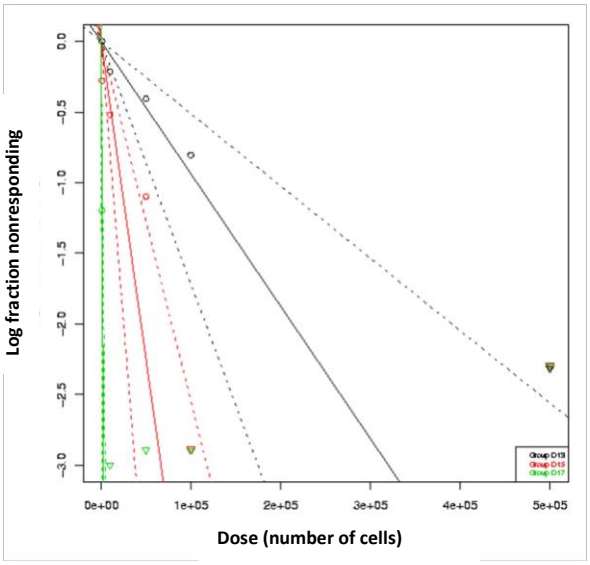

Group	Lower	Estimate	Upper
D13	195415	106723	58285
D15	39318	22258	12600
D17	1448	831	476

Supplementary Figure 6 is related to Figure 7.

Endothelial and hematopoietic potential of D0 to D19 EBs *ex vivo*.

EBs were assessed for their ability to form endothelial or hematopoietic colonies using approved functional assays.

(A) Tubule formation in Matrigel (n=3) and flow cytometry with Ac LDL uptake and hCD31 as a marker (n=3). The highest EC differentiation was found between D7 and D13. Scale bars represent 100µm.

(B) Colony forming units from D0 to D19 EB cells (n=10). CFUs peaked at D17, but the number of hematopoietic cells remained low, indicating weak hematopoietic differentiation. Scale bars represent 200µm

(C) Histograms showing the frequency of CFUs from D0 to D19.

(D) LTC-IC assays were performed with D13 (n=1), D15 (n=1), and D17 (n=1) cells. Confidence intervals of 1/(LTC-IC cell frequency) were calculated using ELDA (http://bioinf.wehi.edu.au/software/elda/) according to Poisson distribution.

Supplemental Tables

	Factor (ng/mL)										Results										
Combination N°	**SCF** (37.38.39.40.e.h)	**TPO** (d)	**FLT3** (37.38.39.40)	**BMP4** (39.40)	**VEGF** (39)	**IL3** (b.d.37.40)	**IL6** (b.d.f.38.40)	**IL1β** (41)	**GCSF** (b.37.38.40)	**IGF1** (36)	**CD90** (e.f.39.41)	**CD109** (a)	**CD13** (c.h)	**CD117** (f.h.39)	**CD38** (b.d.h.36.37.39.41)	**HLA-DR** (h.36.39)	**CD45**	**CD34** (a.b.c.d.e.f.g.h.36.37.38.39.40.41)	**CD33** (c.h)	**LTC-ICs at D16**	**Amplification (Cells at D17/seeded iPSCs)**
1	300	100	20	20	200	5	50	50	10	50	2.39	0.1	0.07	0.44	0.1	0.06	0.41	0.94	0.1	11/1040000	3.01875
2	300	20	300	200	200	50	50	50	10	5	1.11	0.55	0.55	2.34	0.65	0.38	1.92	2.02	0.15	4/640000	1.7325
3	20	20	300	20	200	5	5	5	10	5	1.22	0.24	0.42	1.12	0.44	0.18	0.69	0.96	0.13	6/1390000	5.355
4	300	20	20	200	20	5	50	5	100	5	0.82	1.87	3.09	3.38	1.48	0.66	3.71	4.61	0.97	4/1340000	3.81675
5	20	100	20	20	200	50	50	50	100	5	1.77	1.97	2.66	5.24	2.9	1.01	3.58	5.48	2.2	6/1440000	6.23175
6	20	20	20	200	200	5	5	50	100	5	16.89	1.51	0.69	1.4	0.59	0.83	6.29	10.08	0.59	1/100000	0.462
7	20	100	300	20	20	5	50	5	10	5	3.44	0.28	0.15	1.05	0.31	0.24	0.51	1.14	0.23	1/1040000	3.78
8	300	20	20	20	200	50	5	5	10	50	0.92	1.54	2.71	3.47	1.39	0.62	2.62	4.27	0.63	7/1340000	3.92175
9	300	100	20	20	20	50	5	5	100	5	1.47	0.23	0.22	0.77	0.22	0.14	0.53	1.56	0.16	0	3.07125
10	20	20	20	200	20	50	50	5	10	50	5.22	0.48	0.48	0.68	0.75	0.2	3.99	1.48	0.14	0	1.6485
11	300	100	300	200	20	50	5	50	10	5	0.91	0.75	0.28	1.5	0.16	0.23	1.96	0.51	0.03	0	0.504
12	300	100	300	200	200	5	5	5	100	50	1.28	1.27	0.39	6.34	0.83	0.89	4.98	3.95	0.14	0	0.1785
13	20	20	300	20	20	50	5	50	100	50	1.78	0.34	0.17	0.88	0.19	0.11	0.35	1.45	0.31	3/90000	2.73

14	20	100	300	200	200	50	50	5	100	50	4.43	2.01	2.33	3.76	0.99	0.71	3.71	12.88	0.47	4/70000	0.336
15	300	20	300	20	20	5	50	50	100	50	1.91	0.45	0.39	0.82	0.19	0.2	0.8	1.8	0.28	9/1040000	3.07125
16	20	100	20	200	20	5	5	50	10	50	3.71	0.58	0.8	1.34	0.3	0.21	1.02	2.43	0.07	2/640000	1.87

Supplemental Table 1 related to Figure 1.

Cytokine combinations and cytokine concentrations tested for their ability to promote hematopoietic differentiation. Results after 17 days in terms of cell phenotype, cell amplification and ability to generate LTC-ICs.

	Input (Concentrations in ng/mL)										**Output**							
	SCF	**TPO**	**FLT3**	**BMP4**	**VEGF**	**IL3**	**IL6**	**IL1**	**GCSF**	**IGF1**	**% of CD34$^+$**		**% of CD43$^+$**		**% of CD45$^+$**		**% of CD117$^+$**	
											FD136-25	**IMR90-16**	**FD136-25**	**IMR90-16**	**FD136-25**	**IMR90-16**	**FD136-25**	**IMR90-16**
Combination A	24	21	21	194	200	50	50	5	100	5	3.11	7.49	4.25	10.24	2.24	4.17	4.97	9.47
Combination B	25	27	22	198	196	5	50	6	100	5	5.14	4.15	4.16	3.83	1.6	3.02	6.15	6.42
Combination C	22	20	300	22	200	50	50	5	100	50	6.89	8.53	4.58	3.42	3.99	15.72	7.02	2.82

Supplemental Table 2 related to Figure 1.

Matrix-based three best combinations of cytokines and growth factors and the percentages of CD34$^+$, CD43$^+$, CD45$^+$ and CD117$^+$ obtained with the corresponding combinations.

N°	hiPS	Cytometry/ qRT-PCR	Immunofluorescence	scRNA seq	Functional *ex vivo* assays	First recipients	Flow cytometry qRT-PCR hematopoietic assays	Bone marrow scRNA seq	Second recipients	Flow cytometry qRT-PCR hematopoietic assays	Third recipients	Flow cytometry qRT-PCR hematopoietic assays
DOE												
1	FD136	Yes	No	No	Yes	No	No	No	No	No	No	No
2	IMR90	Yes	No	No	No	No	No	No	No	No	No	No
3	FD136	Yes	No	No	No	9 (NOD SCID)	No	No	No	No	No	No
4	FD136	Yes	No	No	No	6 (NOD SCID)	No	No	No	No	No	No
Kinetic experiments												
5	FD136	Yes	No	No	No	No	No	No	No	No	No	No
6	PC1429	Yes	No	No	Yes	No	No	No	No	No	No	No
7	PCi-CAU	Yes	No	No	Yes	No	No	No	No	No	No	No
8	PC1429	Yes	No	No	Yes	No	No	No	No	No	No	No
9	PCi-CAU	Yes	No	Yes	Yes	No	No	No	No	No	No	No
10	PCi-CAU	Yes	No	Yes	Yes	No	No	No	No	No	No	No
11	PC1429	Yes	Yes	No	No	No	No	No	No	No	No	No
12	PCi-CAU	Yes	Yes	No	No	No	No	No	No	No	No	No
Experiments with NOD SCID												
13	FD136	Yes	No	No	Yes	4	Yes	No	0	No	0	No
14	FD136	Yes	No	No	Yes	8	Yes	No	8	Yes	0	No
15	FD136	Yes	No	No	Yes	8	Yes	No	8	Yes	3	Yes
16	CT-	No	No	No	No	3	Yes	No	3	Yes	3	Yes
Experiments with NSG												
17	FD136	Yes	No	No	Yes	4	Yes	No	4	Yes	No	No
	PC1429	Yes	No	No	Yes	3	Yes	No	3	Yes	No	No
	PCi-CAU	Yes	No	No	Yes	3	Yes	No	3	Yes	No	No
	CT -	No	No	No	No	2	Yes	No	2	Yes	No	No
18	FD136	Yes	No	No	Yes	3	Yes	No	3	Yes	No	No
	PC1429	Yes	No	No	Yes	4	Yes	No	4	Yes	No	No

	PCi-CAU	Yes	No	No	Yes	3	Yes	No	3	Yes	No	No
	CT -	No	No	No	No	2	Yes	No	2	Yes	No	No
19	FD136	Yes	No	No	Yes	3	Yes	No	3	Yes	No	No
	PC1429	Yes	No	No	Yes	3	Yes	No	3	Yes	No	No
	PCi-CAU	Yes	No	No	Yes	4	Yes	No	4	Yes	No	No
	CT -	No	No	No	No	2	Yes	No	2	Yes	No	No
20 LDA	PC1429	Yes	No	No	Yes	30	Yes	No	0	No	No	No
	CT -	No	No	No	No	3	Yes	No	0	No	No	No
21	LAM01.005	Yes	No	No	Yes	3	Yes	No	2	Yes	No	No
	LAM02.002	Yes	No	No	Yes	4	Yes	No	3	Yes	No	No
	CT -	No	No	No	No	1	Yes	No	1	Yes	No	No
22	LAM01.005	Yes	No	No	Yes	3	Yes	No	2	Yes	No	No
	LAM02.002	Yes	No	No	Yes	3	Yes	No	3	Yes	No	No
	CT -	No	No	No	No	1	Yes	No	1	Yes	No	No
23	PCi-CAU	Yes	No	No	Yes	17	Yes	Yes	0	No	No	No
	CT -	No	No	No	No	2	Yes	No	0	No	No	No
24 ABG	PCi-CAU	Yes	No	No	Yes	10	Yes	No	0	No	No	No
	CT -	No	No	No	No	2	Yes	No	0	Yes	No	No
Cord blood sorted $CD34^+$ cells												
25	CD34+	Yes	No	No	Yes	4	Yes	No	4	Yes	No	No
26	CD34+	Yes	No	No	Yes	5	Yes	No	5	Yes	No	No
27	CD34+	Yes	No	No	Yes	4	Yes	No	4	Yes	No	No

Supplemental Table 3 related to Figure 2:

Table summarizing all the experiments performed, the number of animals and the hiPSC cell lines used.

CT: control.

Number of cells	Number of recipients	Number of mice with >1% human cell chimerism
100 000	6	6
50 000	6	6
10 000	6	3
5 000	6	1
1 000	6	0

Supplemental Table 4 related to Figure 4

Limiting dilution assay of D17 cells during primary transplantation.

Graded doses of one hundred thousand to one thousand D17 cells were transplanted into irradiated NSG mice. and the percentage of human CD45+ cells in the BM was analyzed 20 weeks after transplantation (n=6 mice per group). Confidence intervals of 1/(stem cell frequency) were calculated using ELDA (http://bioinf.wehi.edu.au/software/elda/) according to Poisson distribution. The limiting cord blood dilution assay published by Guo et al[(i)] served as a reference.

Gene	Endothelial (EB)		Hematopoietic cells (EB)		Early AGM (CS10)	AGM (CS14-15)
	APLNR+	GJA5+	HE	HSC candidate	HSC	HSC
RUNX1						
HOXA9						
MLLT3						
PTPRC						
SPN						
THY1						
VNN2						
HLF						
SPINK2						
GFI1						
SELP						
STAT5A						
ITGA4						
SVOPL						
EMCN						
ACE						
PROCR						
HOXB9						
LIN28B						
CSF1R						
IL3RA						
HLA-DRA						
SELL						
MSI2						
HEMGN						
PROM1						
CDH5						
IGFBP2						
MEIS2						
NRP2						
SOX17						
GJA5						
IL33						
DKK1						
AGTR2						
ALDH1A1						
CD44						
KCNK17						
BCL11A						
LIN28A						
GAD1						
FGF23						

Legend

No expression

Very low expression/a few positive cells

Low to medium expression

Medium to high expression

Supplemental Table 5 related to Figure 6.

Expression of markers for HSC ontogenesis in the endothelial and hematopoietic cells contained in D17 EBs described in Zeng et al., 2021 [54] and Calvanese et al., 2022 [53].

Additional bibliography:

a. Murray, L.J., Bruno, E., Uchida, N., Hoffman, R., Nayar, R., Yeo, E.L., Schuh, A.C., and Sutherland, D.R. (1999). CD109 is expressed on a subpopulation of CD34+ cells enriched in hematopoietic stem and progenitor cells. Exp Hematol *27*, 1282-1294. 10.1016/s0301-472x(99)00071-5.
b. Terstappen, L.W., Huang, S., Safford, M., Lansdorp, P.M., and Loken, M.R. (1991). Sequential generations of hematopoietic colonies derived from single nonlineage-committed CD34+CD38- progenitor cells. Blood *77*, 1218-1227
c. Gaipa, G., Coustan-Smith, E., Todisco, E., Maglia, O., Biondi, A., and Campana, D. (2002). Characterization of CD34+, CD13+, CD33- cells, a rare subset of immature human hematopoietic cells. Haematologica *87*, 347-356.
d. Yin, A.H., Miraglia, S., Zanjani, E.D., Almeida-Porada, G., Ogawa, M., Leary, A.G., Olweus, J., Kearney, J., and Buck, D.W. (1997). AC133, a novel marker for human hematopoietic stem and progenitor cells. Blood *90*, 5002-5012.
e. Radtke, S., Adair, J.E., Giese, M.A., Chan, Y.Y., Norgaard, Z.K., Enstrom, M., Haworth, K.G., Schefter, L.E., and Kiem, H.P. (2017). A distinct hematopoietic stem cell population for rapid multilineage engraftment in nonhuman primates. Sci Transl Med *9*. 10.1126/scitranslmed.aan1145.
f. Murray, L., Chen, B., Galy, A., Chen, S., Tushinski, R., Uchida, N., Negrin, R., Tricot, G., Jagannath, S., Vesole, D., and et al. (1995). Enrichment of human hematopoietic stem cell activity in the CD34+Thy-1+Lin- subpopulation from mobilized peripheral blood. Blood *85*, 368-378.
g. Gunji, Y., Nakamura, M., Osawa, H., Nagayoshi, K., Nakauchi, H., Miura, Y., Yanagisawa, M., and Suda, T. (1993). Human primitive hematopoietic progenitor cells are more enriched in KITlow cells than in KIThigh cells. Blood *82*, 3283-3289.

h. Gu, R., Wei, H., Wang, Y., Lin, D., Liu, B., Zhou, C., Liu, K., Gong, B., Wei, S., Zhang, G., et al. (2017). The number of CD34+CD38+CD117+HLA-DR+CD13+CD33+ cells indicates post-chemotherapy hematopoietic recovery in patients with acute myeloid leukemia. PLoS One *12*, e0180624. 10.1371/journal.pone.0180624.
i. Guo, B., Huang, X., Lee, M.R., Lee, S.A., and Broxmeyer, H.E. (2018). Antagonism of PPAR-gamma signaling expands human hematopoietic stem and progenitor cells by enhancing glycolysis. Nat Med *24*, 360-367. 10.1038/nm.4477.

CELL PRESS DECLARATION OF INTERESTS POLICY

Transparency is essential for a reader's trust in the scientific process and for the credibility of published articles. At Cell Press, we feel that disclosure of competing interests is a critical aspect of transparency. Therefore, we require a "declaration of interests" section in which all authors disclose any financial or other interests related to the submitted work that (1) could affect or have the perception of affecting the author's objectivity or (2) could influence or have the perception of influencing the content of the article.

What types of articles does this apply to?

We require that you disclose competing interests for all submitted content by completing and submitting the form below. We also require that you include a "declaration of interests" section in the text of all articles even if there are no interests to declare.

What should I disclose?

We require that you and all authors disclose any personal financial interests (e.g., stocks or shares in companies with interests related to the submitted work or consulting fees from companies that could have interests related to the work), professional affiliations, advisory positions, board memberships (including membership on a journal's advisory board when publishing in that journal), or patent holdings that are related to the subject matter of the contribution. As a guideline, you need to declare an interest for (1) any affiliation associated with a payment or financial benefit exceeding $10,000 p.a. or 5% ownership of a company or (2) research funding by a company with related interests. You do not need to disclose diversified mutual funds, 401ks, or investment trusts.

Authors should also disclose relevant financial interests of immediate family members. Cell Press uses the Public Health Service definition of "immediate family member," which includes spouse and dependent children.

Where do I declare competing interests?

Competing interests should be disclosed on this form as well as in a "declaration of interests" section in the manuscript. This section should include financial or other competing interests as well as affiliations that are not included in the author list. Examples of "declaration of interests" language include:

> "AUTHOR is an employee and shareholder of COMPANY."
> "AUTHOR is a founder of COMPANY and a member of its scientific advisory board."

NOTE: Primary affiliations should be included with the author list and do not need to be included in the "declaration of interests" section. Funding sources should be included in the "acknowledgments" section and also do not need to be included in the "declaration of interests" section. (A small number of front-matter article types do not include an "acknowledgments" section. For these articles, reporting of funding sources is not required.)

What if there are no competing interests to declare?

If you have no competing interests to declare, please note that in the "declaration of interests" section with the following wording:

> "The authors declare no competing interests."

CELL PRESS DECLARATION OF INTERESTS FORM

If submitting materials via Editorial Manager, please complete this form and upload with your initial submission. Otherwise, please email as an attachment to the editor handling your manuscript.

Please complete each section of the form and insert any necessary "declaration of interests" statement in the text box at the end of the form. A matching statement should be included in a "declaration of interests" section in the manuscript.

Institutional affiliations

We require that you list the current institutional affiliations of all authors, including academic, corporate, and industrial, on the title page of the manuscript. ***Please select one of the following:***

☒ All affiliations are listed on the title page of the manuscript.

☐ I or other authors have additional affiliations that we have noted in the "declaration of interests" section of the manuscript and on this form below.

Funding sources

We require that you disclose all funding sources for the research described in this work. ***Please confirm the following:***

☒ All funding sources for this study are listed in the "acknowledgments" section of the manuscript.*

*A small number of front-matter article types do not include an "acknowledgments" section. For these, reporting funding sources is not required.

Competing financial interests

We require that authors disclose any financial interests and any such interests of immediate family members, including financial holdings, professional affiliations, advisory positions, board memberships, receipt of consulting fees, etc., that:

(1) could affect or have the perception of affecting the author's objectivity, *or*
(2) could influence or have the perception of influencing the content of the article.

Please select one of the following:

☒ We, the authors and our immediate family members, have no financial interests to declare.

☐ We, the authors, have noted any financial interests in the "declaration of interests" section of the manuscript and on this form below, and we have noted interests of our immediate family members.

Advisory/management and consulting positions

We require that authors disclose any position, be it a member of a board or advisory committee or a paid consultant, that they have been involved with that is related to this study. We also require that members of our journal advisory boards disclose their position when publishing in that journal. ***Please select one of the following:***

☒ We, the authors and our immediate family members, have no positions to declare and are not members of the journal's advisory board.

☐ The authors and/or their immediate family members have management/advisory or consulting relationships noted in the "declaration of interests" section of the manuscript and on this form below.

Patents

We require that you disclose any patents related to this work by any of the authors or their institutions. ***Please select one of the following:***

☒ We, the authors and our immediate family members, have no related patents to declare.

☐ We, the authors, have a patent related to this work, which is noted in the "declaration of interests" section of the manuscript and on this form below, and we have noted the patents of immediate family members.

Please insert any "declaration of interests" statements in this space. This exact text should also be included in the "declaration of interests" section of the manuscript. If no authors have a competing interest, please insert the text, "The authors declare no competing interests."

The authors declare no competing interest

☒ **On behalf of all authors, I declare that I have disclosed all competing interests related to this work. If any exist, they have been included in the "declaration of interests" section of the manuscript.**